# History Matching with Reduced Parameterization and Fast Streamline-based Sensitivities

Master Thesis in Reservoir Mechanics

Center for Integrated Petroleum Research


**Fethia Ibrahim**
Departement of Mathematics
University of Bergen
Bergen, Norway
September 27, 2012

**Abstract**

The main goal of history matching is to construct updated models capable of predicting the future performance of the reservoir more accurately. History matching method requires a solution of inverse problem to minimize the objective function. The main idea of the inverse problem is to find model parameters that best match to the production data. An inverse problem is said to be well-posed if stable and unique solution exists, else the problem is said to be ill-posed. Typically history matching is an ill-posed problem, for which non-unique solution exists. Therefore, regularization by parameterization is applied in this thesis to reduce the number of unknown parameters in order to alleviate the problem of ill-posedness. The parameterization includes two aspects: the parameterization structure determined by the set of bases functions and the corresponding coefficients embedded in the structure. Stepwise estimation strategy of parameterization structure is used to sequentially find new parameterization structure that leads to large decrease in the objective function. There are different approaches that can be used to integrate the geological model to production data. These include amplitude matching, time inversion and generalized travel time inversion (GTTI). GTTI is used in this thesis as it merges the travel time matching with the amplitude matching, in such a way that, it preserves the quasi-linear properties of travel time inversion while using the overall production data. In history matching, different optimization algorithms are applied to minimize the objective function. Levenberg-Marquard optimization method is used in this thesis. It is Guass-newton method with a trust region strategy and modified by adding positive term. The work in this thesis is based on the implementation in [1] and extended using the idea that are presented in [5]. Then the parameterization method is compared with standard method both in the ability to reduce the objective function and in characterizing the permeability field. Simulation results illustrated that the parameterization method showed better performance in reducing the objective function and in characterizing the permeability field for simple cases. But for last case the method did not performed well.

# Preface

## Theses organization

This thesis consists of 5 chapters. In chapter 1 the main ideas of the thesis are presented. In Chapter 2, the basic equations that describe the transport of fluid flow in the porous medium are presented. The properties of reservoirs models are briefly discussed. Single phase and two phase fluid flow models are considered. Numerical method which is used to solve the transport equation is stated. Chapter 3 discusses history matching and inverse problem. Least-square method, Amplitude matching, Travel time inversion and Generalized travel time inversions are briefly discussed. Regularization by parameterization with stepwise strategy is also discussed in this chapter. Finally optimization algorithms, Levenberg-Marquargt and Newton's method, are discussed. Chapter 4 explains streamline based sensitivity calculations and mainly focuses on time of flight, arrival time and time-shift sensitivities. Chapter 5 is concerned with simulations results, conclusions and recommendations.

## Acknowledgements

I would like to express my deep and sincere gratitude to my supervisor Inga Berre for her excellent supervision and help during this work. I would like to express gratitude to my co-superviser Tor Harald Sandve for his invaluable assistance and supervision. I gratefully thank my husband Najmi Hassan and all my family for their support and moral. I really appreciate Engineer Abdulfetah Abdela and Engineer Musa Hayato for their crucial comments and assistance on different aspects of the work.

# Contents

# Chapter 1

## 1 Introduction

A petroleum reservoir is a porous medium that contains hydrocarbons (oil and gas). The main goal of reservoir simulator is to predict future performance of reservoirs. In addition, it finds ways and means of optimization recovery of some of the hydrocarbons. It is crucial for reservoir models to have an accurate description. Rock and fluid properties are the two main characteristics that can describe the reservoir models. A reservoir model typically consists of sets of differential equations together with the appropriate sets of initial and boundary conditions. Thus, a reservoir simulator solves the model equations governing fluid flow in the reservoir with the importance of the available information or data.

According to the [3], the available data about the reservoir can be classified in to static and dynamic. Static data is time-invariant and direct or indirect measurement of reservoir properties such as core analysis, well logs, and 3D seismic data while dynamic data (production data) is the time dependent measurements of flow responses such as pressure, flow rate, tracer responses and data from 4D seismic. Dynamic data is important source for the information about reservoirs and should be used to update the reservoir parameters; the process is referred to as history matching.

Traditionally, the reservoir parameters have been updated manually until satisfactory match is obtained, but this is extremely onerous and time- consuming task for reservoir engineers. Therefore modern approach has been developed in automatic history matching. The most common and widely used approach in the oil industry is based on minimizing the objective function (sometimes called misfit function). The main goal of history matching is to construct updated models capable of predicting the future performance of the reservoir more accurately. Thus, history matching method requires a solution of inverse problem to minimize the objective function. That is typically the objective function is given as the sum of the misfit between the observed data $d_j^{obs}$ and $d_j^{cal}$ over all data points $j = 1, \ldots, Nd$ [1]:

$$\sum_{j=1}^{Nd} w_j (d_j^{obs} - d_j^{cal})^2, \tag{1.1}$$

where $w_j$ is scalar that weighs the influence of each data observation $\mathbf{d}$. The main idea of the inverse problem is to find model parameters that best match to the production data. Typically history matching is an ill-posed problem, for which non-unique solution exists in a sense that many possible combinations of reservoir paramters result in equally good matches to the historical observations. There are also measuring errors, numerical errors and model

error involved in the forward problem, which leads to make the problem unstable solution. Thus, regularization by parameterization method is used in order to make the problem stable. For history matching, forward model is a reservoir simulator that can be used to generate the production response after the reservoir properties and the initial and the boundary conditions are specified [3].

In history matching, optimization algorithm is applied to minimize the objective function. Levenberg-Marquard optimization method is used in this thesis. Streamline based method is a basic tool for history matching and provides unique advantages. It is computationally fast and the sensitivities of production responses can be computed analytically along streamline with a single forward run of simulators. The main idea for streamline based methods is to approximate 3D fluid flow in to 1D transport equations along streamlines. In fact only streamline based sensitivity calculation is considered in this thesis while implicit difference method is used to solve the transport equation.

# Chapter 2

# 2 Fluid flow in porous medium

A petroleum reservoir is a porous medium that contains hydrocarbons (oil and gas). A porous medium consists of a solid material called matrix and the empty space which is called pore space. In fact for fluid flow through it, the pore space should be interconnected. This interconnected pore space is called effective pore space. There are a certain portions of the interconnected pores which may are considered as in-effective pores, for example dead end pores (or blind pores), i.e. pores or channel with only narrow single connection to the interconnected pore space. So that almost no flow occurs through them.

There are also isolated pores, which do not have any contribution. The typical size of reservoir is kilometers in each direction while the pore scale size is millimeters or less. Thus, it is impossible to describe the fluid flow through the whole reservoir based on the microscopic model. Because of the huge difference in scales, the porous medium on macroscopic level is characterized. To be able to describe on macroscopic level, different parameters that describe fluid and matrix properties in porous medium must be defined.

## 2.1 Fluid properties

Fluid possess different properties that play a significant role in every science. The most common properties of fluid are fliud density and viscosity.

**Fluid density** ($\rho$)

In a brief definition, it can be described as the mass of fluid per unit volume. It varies with pressure (P) and temperature (T) according to relations called equations of state in [4]. As stated by [4], the equation for fluid density generally presented as

$$\rho = \rho(p, T). \tag{2.1}$$

For isothermal process (temperature is a constant) the equation of density is only a function of P and equation (2.1) can be rewritten as

$$\rho = \rho(p). \tag{2.2}$$

**Fluid viscosity**($\mu$)

Fluids continue to deform as long as shear stress is applied. The ability of a fluid to resist any deformation is called viscosity. A fluid whose behavior obeys Newtons law of viscosity is called Newtonian fluid. The law states that

the shear force per unit area is proportional to the local velocity gradient. This proportionality constant is called viscosity and defined by

$$\tau = \mu \frac{\partial u}{\partial y},$$

where $\tau$ is the shear stress. For isothermal process, the viscosity equation is a function of $p$

$$\mu = \mu(p). \tag{2.3}$$

## 2.2 Rock properties

It is one of fundamental physical properties of reservoir, and has significant influence in the production of oil in the porous medium. Porosity is one of the most important parameter as it determines the storage capacity of fluid in the reservoir rock. Porosity is defined as the fraction of total volume or (bulk volume) occupied by pore space. In general, it is not the entire pore system that will contribute to fluid flow, only fluid in the connected pores can be displaced from the rocks. Thus, it can be defined as the ratio of the total volume of interconnected pores to the bulk volume of the rock sample,

$$\phi = \frac{V_{p_e}}{V_t}, \tag{2.4}$$

where $V_{p_e}$ is the effective pore volume and $V_t$ is the total volume of the medium.

As it is mentioned above the fluid will flow through interconnected pores medium. In 1856, Darcy Henery did a succession of experiments to investigate the ability of water to flow through a different medium. For one dimensional, horizontal linear flow of an incompressible fluid, he found a simple relationship between flow rate is proportional to a given pressures difference through a given cross sectional area of the medium. According [4], the generalized and differential form of Darcys law is given by

$$\mathbf{u} = -\frac{K}{\mu}(\nabla p - \rho g), \tag{2.5}$$

where $\mathbf{g}$ is gravitational acceleration.

Permeability is another main parameter for reservoir engineers. It is a measure of fluid conductivity of the porous medium. The absolute permeability is a property of the medium which only depends on type of rock not on fluid type. The unit of permeability is Darcy. In general permeability varies both in spatial location and direction of flow (anisotropy). Thus, it can be described by a tensor. If the permeablity field is independent of both spatial lacation and directional flow then, the mediun is called homogenous and

isotropic respectively. For this thesis work, the case where isotropic medium is considerd. That is, the permeablity field is independent of directional flow.

## 2.3 Continuity equation

A basic principle of science and engineering is the conservation of mass. The continuity equation is the expression of this basic principle and it is crucial equation for reservoir engineers to describe the transport of fluid in porous medium. Conservation law says that, the physical quantities such as mass and momentum are conserved; that is neither destroyed nor created. To formulate this law, consider some physical quantity $\Gamma$ in a closed volume $\Omega$, $\mathbf{f}$ is the amount of $\Gamma$ flowing through the boundary surface $\partial\Omega$, $\mathbf{n}$ is the outward unit vector and G is the source or sink term. The conservation law can then be expressed as the following integral equation

$$\int_{\Omega} \frac{\partial \Gamma}{\partial t} dV = \int_{\Omega} G dV - \int_{\partial\Omega} \mathbf{f}.\mathbf{n} ds. \tag{2.6}$$

The divergent theorem together with the fact that the conservation law is valid for an arbitrary volume $\Omega$, leads to the continuity equation

$$\frac{\partial \Gamma}{\partial t} + \nabla.\mathbf{f} = G. \tag{2.7}$$

## 2.4 Single-phase flow

In a single phase flow, only one fluid phase (oil) is presented in pore space (voids) of the porous medium. In fact reservoir consists of water and gas in addition to oil. The governing equations for the single phase flow of a fluid in a porous medium are given by the conservation of mass, Darcys law, and an equation of state to close the system of equation. For the single phase flow, the mass density, $\Gamma$ is given by: $\rho\phi$ and the flux density, $\mathbf{f}$ is given as : $\mathbf{f} = \rho\mathbf{u}$, where $\mathbf{u}$ Darcy velocity, the continuity equation (2.7) becomes

$$\frac{\partial(\rho\phi)}{\partial t} + \nabla.(\rho\mathbf{u}) = G. \tag{2.8}$$

The Darcy velocity $\mathbf{u}$ is given by the Generelazed version of Darcy's law on differential form [2].

$$\mathbf{u} = -\frac{K}{\mu}(\nabla p - \rho\mathbf{g}). \tag{2.9}$$

Equation (2.8) and (2.9) together with equation of state for density(2.2) and viscosity (2.3) forms a closed set of equation for a single phase flow in a porous medium.

## 2.5 Model for multi-phase flow

In reservoir simulation, we are often interested in the simultaneous flow of two or more fluid phases within a porous medium. Therefore, basic equations for multiphase flow in a porous medium are developed. In this section, only two-phase flow where the fluids are immiscible is considered. When two fluids are simultaneously presented, the ability of flow of one fluid depends on the local configuration of the other fluid. Thus, some basic physical parameters must be introduced.

### 2.5.1 Basic definitions

#### Saturation

The saturation of a fluid phase is defined as the fraction of the void volume of a porous medium occupied by the fluid that is,

$$S_\alpha = \frac{V_\alpha}{V_{e_p}}, \tag{2.10}$$

where $V_\alpha$ is the volume occupied by phase $\alpha$, where $\alpha$ is represents for oil and water and $V_{e_p}$ is the effective pore volume .

#### Capillary pressure

Capillary pressure can be defined as the pressure difference between the two phases

$$P_c = p_{nw} - p_w, \tag{2.11}$$

where $p_{nw}$ is the pressure in the non wetting phase and $p_w$ is the pressure in the wetting phase. Empirically, the capillary pressure is a function of saturation of wetting phase, $s_w$.

#### Relative permeablity

When two immiscible fluids flow simultaneously, only one immiscible fluid flow through the pore space at a given time, thus the other presented phase reduces the pore space and influences the permeability. Relative permeability is defined as the ability of one fluid flow with respect to the other phase fluid. The effective permeability of each phase fluid is given by

$$k_w = \ K_{rw}K$$

$$K_{nw} = K_{rnw}K,$$

where $K_{rw}$ and $K_{rnw}$ are relative permeablty of wetting fluid and non-wetting fluid .

The Darcy's law for a single phase can be directily extended to multiphase flow.That is

$$\mathbf{u}_\alpha = -\frac{K_\alpha}{\mu_\alpha}(\nabla p_\alpha - \rho_\alpha \mathbf{g}\ ). \tag{2.12}$$

The above eq(2.12) can be expressed as

$$\mathbf{u}_\alpha = -\lambda_\alpha K(\nabla p_\alpha - \rho_\alpha \mathbf{g}), \tag{2.13}$$

where $\lambda$ is mobility and it is defined as

$$\lambda_\alpha = \frac{K_{r\alpha}}{\mu_\alpha}. \tag{2.14}$$

The modified form of the continuty equation (2.8) is

$$\frac{\partial(\rho_\alpha \phi S_\alpha)}{\partial t} + \nabla.(\rho_\alpha u_\alpha) = G_\alpha \tag{2.15}$$

The modified equation(2.15) and the Darcy's equation (2.12) forms a coupled set non-linear differntial equstions. Together with the equation of state, (2.2) and viscosity (2.3) the capillary equation(2.11) and togther with the assumption that the two fluids fill the void space completely, that is $\sum_\alpha S_\alpha = 1$ forms a closed set of equation. Considering initial and boundary condition, it is possible to solve the equations. In practice numerical method can be used to solve the differential equation. Infact analytic solution can be also found for the simplified equation with simple boundaries. In this thesis the simplified model for two phase flow due to Buckley and Leverett will be used.

## 2.6 Buckley-Leverett model for two phase flow

Buckley and Leverett (1942) solved the simplified governing model equation for two phase fluid flow in porous medium with the assumption that it is incompressible, immiscible( there is no mass transfer between phases), constant viscosity, neglecting the effect of gravity and capillary pressure. For constant $\rho$ and $\phi$ equation(2.15) can be rewrite as [1]

$$\phi \frac{S_\alpha}{\partial t} + \nabla.\mathbf{u}_\alpha = \frac{G_\alpha}{\rho_\alpha}. \tag{2.16}$$

The total velocity for the two phase is defind as $\mathbf{u} = \mathbf{u}_o + \mathbf{u}_w$ and with the assumption that the two fluids fill the void space completely, the above equation becomes

$$\phi \frac{\partial}{\partial t}(S_o + S_w) + \nabla.(\mathbf{u}_o + \mathbf{u}_w) = G, \tag{2.17}$$

where $G = \frac{G_o}{\rho_o} + \frac{G_w}{\rho_w}$, and from the assumption, we have $S_w + S_o = 1$. Thus, equation (2.17) is reduced to,

$$\nabla.\mathbf{u} = G. \tag{2.18}$$

Negelecting the gravity, the following expression can be found from Darcy,s law (2.9)

$$\nabla p = \frac{-u_w}{\lambda_w K} \tag{2.19}$$

$$\nabla p = \frac{-u_o}{\lambda_o K}. \tag{2.20}$$

By combining equation (2.19) and (2.20) and using $\mathbf{u}_o = \mathbf{u} - \mathbf{u}_w$, the following expression can be found.

$$\mathbf{u}_w = F_w \mathbf{u}, \tag{2.21}$$

where $F_w$ is fractional flow and is defined as, $F_w = \frac{\lambda_w}{\lambda_t}$ and $\lambda_t$ is the total mobilty given by; $\lambda = \lambda_w + \lambda_o$.
Equations for water saturation is

$$\phi \frac{\partial S_w}{\partial t} + \nabla.(F_w \mathbf{u}) = G, \tag{2.22}$$

where $G = \frac{G_w}{\rho_w}$. For incompressible fluid flow, $\nabla.(F_w\mathbf{u}) = \mathbf{u}.\nabla F_w$ and $\nabla.\mathbf{u} = 0$ way from the wells . The saturation equation is then rewrite as

$$\phi \frac{\partial S}{\partial t} + \mathbf{u}.\nabla F = G. \tag{2.23}$$

And equation (2.18) is

$$\nabla.\mathbf{u} = G, \tag{2.24}$$

where the velocity, $\mathbf{u}$ is given by the Darcy's law with out the gravity term

$$\mathbf{u} = -K\lambda_t \nabla p. \tag{2.25}$$

The equation (2.24) and (2.23) are called elliptic pressure equation and the hyperbolic transport equation respectively. There are different numerical method to solve these equation and clearly mentioned in the [16]. One way of solving the differential equation is to discretize using the Finite differnce method and solve them based on implicit Schemes, which is used in this thesis. we apply reservour simulator, which is called MRST. To get detail valuable understanding how the analysis of this shceme applied in practise refer to [16]. Infact in the next section, the concept of implicite scheme and explicit scheme will be introduced.

## 2.7 Finite difference method

As it is known that , fluid flow in porous medium involves large, coupled system of non linear time dependent differential equations, it is reasonable to consider numerical methods that gives stable, efficient and accurate solutions. Consider the general hyperbolic model differential equation [16] given that,

$$\frac{\partial p}{\partial t} + b\frac{\partial p}{\partial x} = 0. \tag{2.26}$$

where $b$ is constant and initial condition given as

$$p(x, o) = p_o(x).$$

In order to solve the above problem numerically three different techniques (approaches) are used. These are Forward Difference, Backward Difference and Central Difference (approaches) techniques.

### 2.7.1 Forward difference

**For implicite scheme,**

Implicite method are the technique in which it can compute the next state of the system by solving a equation involving both current state and next state. The hyperbolic equation (2.26), can be discretized as

$$\frac{P_i^{n+1} - P_i^n}{\Delta t} + b\frac{P_{i+1}^{n+1} - P_i^{n+1}}{h} = 0, \tag{2.27}$$

where P is a discrete function of time and space, $'n'$ is the time step index. It is important to define amplification factor to analyse the stabilty of this approach. Assume that, there is an error $\varepsilon^n$ that occur at time step$'n'$. The amplification factor of this at time step n+1 can be define as

$$\varepsilon^{n+1} = \gamma\varepsilon^n, \tag{2.28}$$

where $\gamma$ is the amplification factor. It is clearly derived how to solve the amplication factor in [16]. Based on this, the amplication factor can be expressed as

$$\gamma = \frac{\gamma^{n+1}}{\gamma^n}. \tag{2.29}$$

The Von Neumann criterion for stability is that the modulus of this factor should not be greater than one, that is

$$|\gamma| \leq 1 \tag{2.30}$$

In general, the simple method for finding the stability criterion is to construct Fourier analysis of difference equation and derive the ampliction factor. Therefore, the stability analysis of the finite diffence method for the equation (2.27), can be expressed as

$$\gamma = \left(1 - \frac{b\Delta t}{h}\left(1 - cos(kh)\right) + i\frac{-b\Delta t}{h}sin(kh)\right)^{-1}. \tag{2.31}$$

Thus, for the stabilty $|\gamma| \leq 1$, the above equation becomes

$$|\gamma|^2 = \left(1 - 4\frac{b\Delta t}{h}sin^2\left(\frac{kh}{2}\right)\left(1 - \frac{b\Delta t}{h}\right)\right)^{-1} \leq 1. \tag{2.32}$$

Inequality (2.32), is satified if $b < 0$. Therefor, the scheme (2.27), is unconditionally stable when $b < 0$.

**For explicit scheme,**

Explicite method are the technique in which it can compute the next state of the system intems of current state. The hyperbolic equation (2.26), can be represented as

$$\frac{P_i^{n+1} - P_i^n}{\Delta t} + b\frac{P_{i+1}^n - P_i^n}{h} = 0, \tag{2.33}$$

where P is function of time and space and $'n'$ is the time step.
Similarly, the stability criterion of the explicit forward difference scheme will be satisfied when $b < 0$ and with condition given below:

$$\frac{|b|\Delta t}{h} \leq 1 \tag{2.34}$$

The above Inequality is called the Courant-Friedrichs-Lewy (CFL) condition. Thus, the Forward difference scheme (2.34) is conditionlly stable if $b < 0$. Eventhough the expilcit method is computationally efficient, it reqiures the CFL condition should be satisfied for each iteration.This makes the expilcite method is infeasible in practical simulation.

### 2.7.2 Backward difference

**For implicite scheme,**

By applying the same argument as the above, the Backward difference for hyperbolic equation can be written as

$$\frac{P_i^{n+1} - P_i^n}{\Delta t} + b\frac{P_i^{n+1} - P_{i-1}^{n+1}}{h} = 0. \tag{2.35}$$

A similar argument is used to prove that the shceme (2.35) has the same stability property as the scheme(2.27) when $b > 0$ .

**For explicite scheme,**

In this case, the hyperpolic eqaution can be represented as

$$\frac{P_i^{n+1} - P_i^n}{\Delta t} + b\frac{P_i^n - P_{i-1}^n}{h} = 0. \tag{2.36}$$

For the explicit difference scheme, it has the similar stability property as the scheme(2.33) when $b > 0$ given that,

$$\frac{|b|\Delta t}{h} \leq 1. \tag{2.37}$$

### 2.7.3 Centeral difference

**For implicite scheme,**

The centered difference formulation of the above problem(2.26) is,

$$\frac{P_i^{n+1} - P_i^n}{\Delta t} + b\frac{P_{i+1}^{n+1} - P_{i-1}^{n+1}}{2h} = 0. \tag{2.38}$$

The amplification factor $\gamma$ of the centered difference approach is given as

$$\gamma = \left(1 + i\frac{-b\Delta t}{h} sin(kh)\right)^{-1}. \tag{2.39}$$

which always satisfy the inequalty $|\gamma| \leq 1$. Hence for all values of b, this scheme is unconditionally stable.

**For explicite scheme,**

$$\frac{P_i^{n+1} - P_i^n}{\Delta t} + b\frac{P_{i+1}^{n+1} - P_{i-1}^{n+1}}{2h} = 0. \tag{2.40}$$

In contrast to implicit, the expicity difference scheme is always unstable.

# Chapter 3

# 3 History matching

In this chapter, the concept of history matching, and its advantage and challenges will be discussed. Amplitude matching, travel time inversion and generalized travel time inversion (GTTI) will be introduced. History matching plays a significant role in characterizing the reservoir accurately. This helps reservoir engineers to predict future performance of the reservoir. The major goal of history matching is to find the reservoir parameter that minimizes the misfit between the calculated data and observed production data. There are different parameters that can be considered for history matching, such as permeability, relative permeability and porosity. Similarly, some of the dynamic data that are considered for history matching are pressure and water cut data. Permeability is the parameter to be considered in this work for the history matching problem. Likewise watercut data is used in parameter estimation.

The main challenge in history matching is that history matching is an inverse problem which is typically ill-posed due to limited amount of available information. Morever the governing equations for fluid flow in porous medium are nonlinear. In another way, the relationship between reservoir parameter and production response is nonlinear. These make it more challenging in solving the system of equations. Therefore, solving inverse problem needs carefully analysis. An inverse problem is said to be well possed if stable and uniques solution exists, else the problem is said to be ill-posed. The overview of inverse problem will be presented in the next section.

## 3.1 Inverse problem

The main goal of reservoir simulator is to predict future performance about the reservoir. In general, it is possible to predict data from a given model through physical laws. This is called Forward problem,

$$\mathbf{G}(\mathbf{m}) = \mathbf{d}, \tag{3.1}$$

where $\mathbf{m}$ is model parameter, $\mathbf{d}$ is the observed data set, and $\mathbf{G}$ is the operator that relates $\mathbf{m}$ and $\mathbf{d}$. Model is a set of parameters which describes the physical properties of the system. In reality, some amount of noise present in the actual observation data.This noise may arise from instrumental reading during observation or numerical round off. Thus, the observed data is $\mathbf{d} = \mathbf{d}_t + \eta$. For linear problem, the matrix equation (3.1) can mathematically be represented as

$$\mathbf{Gm} = \mathbf{d}. \tag{3.2}$$

where G $\in \mathbb{R}^{m\times n}$, d $\in \mathbb{R}^{m\times 1}$ and m $\in \mathbb{R}^{n\times 1}$. In contrast to the forward problem, the main target of inverse problem is to find model **m** for a given data **d**. History matching problem is an example of inverse problem, where it consists of adjusting a set of parameters in order to match the predicted data to the actual production data. There are two main approaches to formulate inverse theory, deterministic and stochastic. The main focus of this section will be on deterministic approach. Solution strategies based on deterministic approach will be presented later in this chapter. In the presence of measurement, model and numerical error, the observed data will not fit any model or fit infinitely many model. Therefore, careful analysis needs to be done in order to find optimal and unique solution. There is a method that finds a model that minimizes the objective function. This is called least square method and the model is called least square solution.

## 3.2 Least-square method

Least square method is a standard approach to approximate solution of over determined system. This is the case when there are more data than model parameters. For over determined system of full rank, the solution will be unique but not exact. It is possible to find a model that minimizes the objective function rather than the exact solution. The objective function **f** is defined in terms of $L_2$ norm

$$f(\mathbf{m}) = \| \ \mathbf{r} \ \|_2^2 = \sum r_i^2, \tag{3.3}$$

where **r** is residual, $\mathbf{r} = \mathbf{Gm} - \mathbf{d}$. Minimization problem (3.3) is used to find a solution for inverse problem.There are different numerical approaches to solve nonlinearity in inverse problem, which will be considered later in this chapter. In history matching, there are different approaches that can be used to integrate the geological model to production data. These includes amplitude matching, time inversion and generalized travel time inversion (GTTI).

## 3.3 Amplitude matching

Amplitude matching is traditional approach that is used to match the amplitude of production history directly. The main challenge of amplitude matching is that, it is highly non-linear inverse problem which is difficult to converge. The least square formulation for amplitude matching is given by

$$\sum_{k=1}^{Nw}\sum_{i=1}^{Nd}(d_k^{obs}(t_{k,i}) - d_k^{cal}(t_{k,i}))^2. \tag{3.4}$$

where $d_k^{obs}(t_{k,i})$ and $d_k^{cal}(t_{k,i})$ are the simulated(calculated) and obseved data respectively. This is minimized for all time $t_{k,i}$.where the time index $j$ =

$1, 2, \ldots, N_d$ and the well index $k = 1, 2, \ldots, N_w$.

### 3.4 Travel-time inversion

The basic idea of the travel time inversion is that the production data at a given reference time such as breakthrough time or the first arrival time can be matched. The main advantage of travel time inversion is that, it has the quasi-linear properties. This makes the travel time inversion more stable and robust than amplitude matching. However, the travel time inversion only requires production data at a given time. To incorporate all amplitude data while retaining the properties of the travel time inversion, the generalized travel time inversion is introduced.

### 3.5 Generalized travel-time inversion (GTTI)

The basic idea of generalized travel time inversion is to merge the travel time matching with the amplitude matching, in such a way that, GTTI preserves the quasi-linear properties of travel time inversion while using the overall production data [6]. GTTI approach solves the problem by systematically shifting the calculated production response towards the observed response in small increments. Then, the data misfit is computed for each time increment. Consequently, generalized travel time inversion solves the history matching problem in two steps: Firstly, it finds the optimal time-shift that minimizes the objective function given by

$$f(\Delta t_k) = \sum_{i=1}^{Nd} (d_k^{obs}(t_{k,i}) - d_k^{cal}(t_{k,i} + \Delta t_k))^2. \tag{3.5}$$

For all k. The above least square problem can be solved systematically shifting the calculated production curve until the objective function is minimized. Secondly, it minimizes the following equation

$$\sum_{i=1}^{Nd} \Delta t_k^2. \tag{3.6}$$

The advantage of GTTI is that the relation between the reservoir parameter and the time-shift is less-nonlinear than the direct relation between amplitude of production data. The least square problem in (3.6) is solved with the algorithm for solving nonlinear least square problem[1].

As it was discussed in section (3.1) inverse problems are ill posed. To obtain a meaningful solution and alleviate the problem of ill- posedness, a regularization strategy is necessary to stabilize the solution of the inverse problem. Two main approaches for regularization are commonly applied, The approaches differ based on whether or not the set of admissible estimates is

constrained directly by modifying the parameter space, or if it is constrained indirectly by modifying the inverse estimator [4]. In this paper, the former approach is used which is called regularization by parametrization.

### 3.6 Regularization by parameterization

One way of regularizing the problem is reducing redundancy by replacing the set of unknowns spatially discretized the reservoir properties by small number of parameters that can capture the most important features of the field. The process is called parameterization. By using parameterization with stepwise strategy process, it is possible to obtain representation of permeability field . A parameterization includes two aspects: the parameterization structure determined by the set of basis functions and the corresponding coefficients embedded in the structure. For linear parameterization of unknowns, discrete permeability field can then be represented as

$$\mathbf{P} = \mathbf{SC}, \tag{3.7}$$

where $\mathbf{p}$ is permeability field, $\mathbf{C} = [\mathbf{c}_1\mathbf{c}_2 \dots \mathbf{c}_n]^\intercal$ are coefficient vectors, $\mathbf{S} = [\mathbf{s}_1\mathbf{s}_2 \dots \mathbf{s}_n]$ is the $m \times n$ structural matrix ($m >> n$) and $s_1, s_2, \dots s_n$ are base vectors. In general, the permeability distribution can vary in a manner determined by the shape and support of the basis vectors. In the parameterization (3.7), the identification of $\mathbf{p}$ is replaced by identification of coefficient vector $\mathbf{c}$ . Hence, during optimization process and sensitivity calculation, the coefficient vector is considered.

Common choices of paramterization structure are zonation, pilot points and the other interpolation techniques. In this thesis, an approach where base vectors that corresponds to discretized radial basis function (RBF) for parameterization of permeability field is considered. Gaussian RBF is used for the results that will be presented. Gaussian RBF is then given by

$$\mathbf{S}_i = exp(-\frac{1}{2\sigma_i^2}(x - x_i)^2), x_i \in B, \tag{3.8}$$

where $'B'$ denots the position of knots (base points) and $\sigma_i$ is the parameter shape. Stepwise estimation strategy and performance measurement are basic concepts which help to update the structural matrix in a sense that by selecting the best basis vectors among the possible choices.

### 3.7 Stepwise estimation strategy

The main idea of stepwise estimation strategy is to sequentially find new parameterization structure that leads to large decrease in the objective function. At each stage of stepwise strategy one or few basis vectors are added

to the structure. The new parameter space will then have higher dimension. This new parameter space includes the previous one, which results in a sequence of nested parameter space. This satisfies,

$$span(\mathbf{S_1}) \subset span(\mathbf{S_2}) \subset span(\mathbf{S_3}) \subset \ldots .,$$

where $span(\mathbf{S_i}) = span(\mathbf{s_1}, \mathbf{s_2}, \ldots, \mathbf{s_n})$ denotes the column space of $S_i$ . At the beginning of each stages, one or few basis vectors are selected from the set of possible choices based on performance measure and added to the parameterization structure. Then the new estimation is started with the result from the previous estimation as initial state. This process will continue until the convergent criteria is met. The flow chart in fig. (1) illustrate the process breifly.

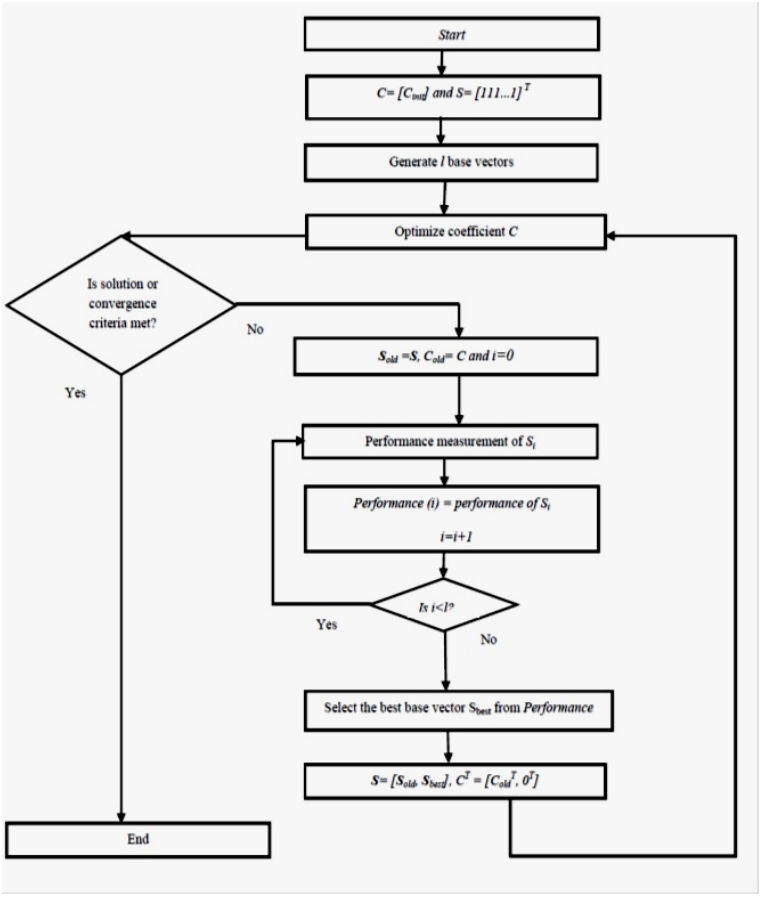


Figure 1: Flow chart for stepwise estimation procedure to update the parametrizatio structure

## 3.8 Performance measure

There are two approach that are used to estimate the tentative performance of the parameterization structure. The first approach is, the objective function gradient and the other is linearization of the model response. In this work the first approach is used for the performance measurement. The objective function gradient gives for the representation to the steepest descent direction in solving minimization problem. By considering the norm of the objective gradient, one can analyze the effectiveness of coefficient values that corresponds to the refined structure. This norm implies a measure of how sensitive the objective function is to change in coefficient vector which corresponds to a new structure. The norm which has the greatest value will be taken to choose the basis vectors for the representation.

## 3.9 Optimization method for solving non-linear inverse problem.

In section (3.6) how to regularize inverse problem based on parameterization approach have been shown. Optimization technique that solves nonlinear inverse problem will be considered in this section. The main task is that to find the parameter that gives optimal solution. One approach is to use local Taylor approximation of the objective function iteratively at the point at which the objective function is smaller than the surrounding points. This is local solution, not the global. In fact global solution is essential in some application, but it is difficult to find the solution [11]. The optimization algorithm which is presented in this paper is Levenberg-Marquardt which is a local solver.

#### Levenberg-Marquargt method (LM)

To come up into insight explanation on LM method, first let's introduce line search, trust region and scaling strategies along with Newtons method and Gauss Newtons method for solving minimization problem.

### 3.9.1 Line search, trust region and scaling strategies

In the line search strategy, the main approach is to choose some direction pk and searches for the next iterate $x^{x+1}$ along this direction from the current iterate $x^k$ such that the new iterate will have a lower function value. The step length can be found by solving the following optimization problem,

$$min_{\alpha>0} f(x^k + \alpha p_k),$$

where $\alpha$ is step length and $p_k$ is the direction. A trust region strategy is based on constructing a trust region where the solution is searched within.

The trust region sub-problem can be formulated as

$$\min_{\mathbf{m}} f(\mathbf{m}) such that ||\mathbf{m}|| \leq \Delta k.$$

The trust region radius $\Delta k$ is chosen based on the performance of the previous iterations. There are different algorithm that computes the trust region refer [11].

The performance of an algorithm may depend crucially on how the problem is formulated. One important issue in problem formulation is scaling. In unconstrained optimization, a problem is said to be poorly scaled if changes to x in one direction produce much larger variations in the value of **f** than do change to x in another direction. One way to scale the problem is to use a ellipsoidal trust region instead of a spherical trust region. The trust region sub-problem then becomes

$$\min_{\mathbf{m}} f(\mathbf{m}) such that ||\mathbf{D}^k \mathbf{m}|| \leq \Delta k, \tag{3.9}$$

where $\mathbf{D}^k$ is a diagonal matrix where the diagonal elements are the principal axes of the trust region.

### 3.9.2 Newton's method

Given initial $\mathbf{m}^0$, the algorithm generate a sequence of vector$(\mathbf{m}^1, \mathbf{m}^2, ..)$ iteratively until it will converge or no more progress can be made. If f is twice continuously differentiable, the nonlinear objective function f can be approximated using Taylor series approximation around $\mathbf{m}^k$,

$$f(\mathbf{m}^k + \Delta\mathbf{m}) \approx f(\mathbf{m}^k) + \Delta\mathbf{m}^\intercal \nabla f(\mathbf{m}^k) + \Delta\mathbf{m}^\intercal \nabla^2 f(\mathbf{m}^k) \Delta\mathbf{m}, \tag{3.10}$$

where $\nabla f(\mathbf{m}^k)$ and $\nabla^2 f(\mathbf{m}^k)$ are the gradient and the Hessian of $f(\mathbf{m}^k)$ respectively. To get the minmum value $\mathbf{m}*$ for the objective function, the gradient must be zero, then it can be approximate the gradient of $f(\mathbf{m}^k + \Delta\mathbf{m})$ about $\mathbf{m}^k$,

$$\nabla f(\mathbf{m}^k + \Delta\mathbf{m}) \approx \nabla f(\mathbf{m}^k) + \nabla^2 f \mathbf{m}^k) \Delta\mathbf{m}. \tag{3.11}$$

By approximating the gradient equal to zero, a local minimum of the objective function can then be found by solving the following equation,

$$\nabla^2 f(\mathbf{m}^k) \Delta\mathbf{m} \approx -\nabla f(\mathbf{m}^k), \tag{3.12}$$

where this solves for successive solution steps until it convergence see the detail [12].

For least square problem, the gradient of objective function can be written in marix notation interms of jaccobian of $\mathbf{r}(\mathbf{m})$ see [11 ]

$$\nabla f(\mathbf{m}) \approx \mathbf{J}(\mathbf{m})^\intercal \mathbf{r}(\mathbf{m}). \tag{3.13}$$

Similarly, the Hessian is,

$$\nabla^2 f(\mathbf{m}) \approx \mathbf{J}(\mathbf{m})^\intercal \mathbf{J}(\mathbf{m}) + \sum_{j=0}^{m} \mathbf{r}_j(\mathbf{m}) \nabla^2 \mathbf{r}_j(\mathbf{m}). \tag{3.14}$$

In many application, it is possible to calculate the Jacobian matrix expicitly where as to find the Hessian of $f(\mathbf{m})$ explicitly are often not possible. In newtons method, the Hessain of f $f(\mathbf{m})$ must be calculated in each iteration which is often computationally expensive. There is an optimization method developed which ignores the last part of the Hessian which is $\nabla^2 f(\mathbf{m}) = \mathbf{J}(\mathbf{m})^\intercal \mathbf{J}(m)$. This method is called Guass-Newtons method. Then equation (3.12) beomes,

$$\mathbf{J}(\mathbf{m}^k)^\intercal \mathbf{J}(\mathbf{m}^k) \Delta \mathbf{m} \approx -\mathbf{J}(\mathbf{m}^k)^\intercal \mathbf{r}(\mathbf{m}^k). \tag{3.15}$$

Even though Guass-newtons method is the modification of newtons method and it works well in practice. The method fails when the matrix $\mathbf{J}(\mathbf{m}^k)^\intercal \mathbf{J}(k)$ is singular. Therefore, there is a method called Levenberg-Marquargt method (LM) which modifies GN.

### 3.9.3 Levenberg-Marquardt method

A Guass-newton method with a trust region strategy is called LM method. A GN method is then modified by adding positive term, $\lambda I$ to (3.15). The LM method is then represented as

$$(\mathbf{J}(\mathbf{m}^k)^\intercal \mathbf{J}(\mathbf{m}^k) + \lambda \mathbf{I}) \Delta \mathbf{m} \approx -\mathbf{J}(\mathbf{m}^k)^\intercal \mathbf{r}(\mathbf{m}^k) \tag{3.16}$$

The positive parameter that is added, is adjusted during the course of algorithm to ensures convergence, the reason for using positive value of $\lambda$ is that the term $\lambda \mathbf{I}$ enures that the matrix is non singular. The paramter $\lambda$ is closely related to the trust radius since it always a positve $\lambda \mathbf{I}$ exits such that equation (3.16) and (3.9) satified. For large $\lambda$, the algorithm simply moves to the steepest-desent direction rapidly in a sense of reducing the objective function. The steepest-desent direction provides convergence if a certain steps are taken. Conversely for small value of $\lambda$, the LM method reverts to the GN [12].

As it is mentioned in section (3.9.1), the scaling startegy can be applied on Lm method. One way is to use ellipsoid trust region instead of spherical trust region. Thus, the problem (3.16) is modifies to

$$(\mathbf{J}(\mathbf{m}^k))^\intercal \mathbf{J}(\mathbf{m}^k) + \lambda^k ((\mathbf{D}^k)^\intercal \mathbf{D}^k) \Delta \mathbf{m} \approx -\mathbf{J}(\mathbf{m}^k)^\intercal \mathbf{r}(\mathbf{m}^k). \tag{3.17}$$

# Chapter 4

# 4 Streamline based sensitivity calculation

The basic advantage of streamline based sensitivity calculation is that the sensitivities can be computed semi-analytically along the streamline.This makes it to have the ability of efficiently (fast) computing the sensitivity of the production data to reservoir parameters for high-resolution geological models. In addition, the computation of sensitivity for all model parameters requires a single simulation run. The computations of sensitivities are based on the assumption that the streamlines do not shift during perturbation. But first some basic concept will be introduced.

## 4.1 Fundemental definition

### 4.1.1 Streamline

Streamlines are instantaneous lines that are everywhere tangential to the direction of velocity. Mathematically can be defined as a function of $\mathbf{x}$ that solves differential equation

$$d\mathbf{x} \times \ \mathbf{u}\left(\mathbf{x}, t_0\right) = 0, \mathbf{x}\left(t_o\right) = \mathbf{x}_o, \tag{4.1}$$

where $\mathbf{u}$ is the velocity field. A streamline is generated by defining a starting point( initial position ) commonly referred to as a seed point, and the velocity field at that instant in time. If the velocity field is steady state (time independent), streamline are related to path line. path line is physical trajectory of a single particle through time and space. But as in the case of unsteady state problem where the velocity field varies through time, streamlines represents the instantaneous velocity, not physical trajectory. In addition to this, pathlines may often cross each other, but streamlines does not. Therefore, there is no mass transfer between each fuid particles.

### Streamfunction

Streamfunctions are scalar quntities whose main advantage is to define streamlines by constant values of streamfunction. That means, the contour line of this scalar function is given as streamlines, which represent the trajectories of particles in a steady flow. It is possible to illustrate this by considering streamfunction in 2D.

### Streamfunction in 2D

In addition to determining the fluid velocity from Darcys equation and the gradient of pressure equation, it is also possible to determine from the deriva-

tive of streamfunction $\Psi$. For 2D flow of incompressible fluid describing a function $\Psi$ in Cartesian coordinate system, the velocity can be represents as

$$\begin{aligned} u_x &= \frac{\partial \Psi}{\partial y} \\ u_y &= -\frac{\partial \Psi}{\partial x}, \end{aligned} \tag{4.2}$$

where $u_x$ and $u_y$ are the velocities in the x and y coordinate.

The definition of streamline in equation(4.1) in xy plane simplifies into

$$\frac{dx}{u_x} - \frac{dy}{u_y} = 0. \tag{4.3}$$

By substitute eq(4.2) into (4.3) gives as

$$\frac{\partial \Psi}{\partial x} dx + \frac{\partial \Psi}{\partial y} dy = 0. \tag{4.4}$$

The above solution implies that $\Psi(x, y)$ is constant along streamline. From the above derivation, it can be observed that the streamfunction and streamline are related in a such way that, a line given by constant streamfunction $\Psi$ is defined streamlines.

### Streamfunction in 3D

The concept of streamfunction in 2D can be visualized(extended) into 3D flow. It repersents two family of surface whose intersection define streamline [3 ]. Following Bear( 1972), for divergence free flow and incompressible fluid, the velocity field in 3D can be represented intermes of two scalar functions $\psi$ and $\chi$ is

$$\mathbf{u} = \nabla\psi \times \nabla\chi, \tag{4.5}$$

where $\psi$ and $\chi$ are bi-streamfunctions.
Following the above definition, the continuity equation is

$$\nabla.(\nabla\psi \times \nabla\chi) = 0. \tag{4.6}$$

Since the cross product of must lie in both surfaces, their intersection defines streamline. Bi-Streamfunctions have significant role for time of fight coordinate system.

### 4.1.2 Time of flight

Time of flight is the travel time of passive particles along streamline. For steady state, streamline are traced out by following the physical trajectory of passive particles with in a reservoir, so that the velocity field $\mathbf{u}$ is tangential to streamline at every point along streamline. According to [3] time of flight $\tau$ along streamline $\Gamma$ is represented as

$$\tau = \int_{\Gamma} \frac{\phi}{|\mathbf{u}|} d\xi, \tag{4.7}$$

where $d\xi$ is spatial coordinate.

### 4.1.3 Pollocks method for tracing streamlines

To use streamline time of flight as spatial coordinate is a unique feature for streamline simulation. Thus it is important to consider the computation of time of flight. It is common to use the semi-analytical Pollocks method to obtain streamline and time of flight in 3 dimensional regular grid blocks. For every grid cells, Pollocks method is assumed piece wise linear approximation of velocities in each direction. The velocities are given as

$$\begin{aligned} u_x &= u_{x1} + c_x\,(x - x_1)\,; \\ u_y &= u_{y1} + c_y\,(y - y_1)\,; \\ u_z &= u_{z1} + c_x\,(z - z_1)\,, \end{aligned} \tag{4.8}$$

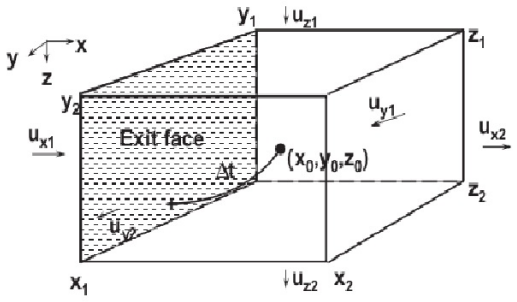


Figure 2: Pollock's construction of streamline

where $(x_1, x_2, y_1, y_2, z_1, z_2)$ are the corners in the cell and $(u_{x1}, u_{x2}, u_{y1}, u_{y2}, uz_1, u_{z2})$ are fluid velocities on each of the six faces of the cell see **Figure**(2). These velocities on the faces s are usually provided by solving pressure equation (2.24) numerically. The coefficients are found directly from the differences of the Darcy's velocities on each of the cell faces

$$c_x = \frac{(u_{x2} - u_{x1})}{(x_2 - x_1)}, c_y = \frac{(u_{y2} - u_{y1})}{(y_2 - y_1)}, c_z = \frac{(u_{z2} - u_{z1})}{(z_2 - z_1)}. \tag{4.9}$$

For incompressible fliud flow, we have $\nabla.u = 0$. By applying this to equation ( 4.8) becomes

$$c_x + c_y + c_z = 0. \tag{4.10}$$

The above eq(4.10) implies that for an incompressible flow, the discrete solution conserves flux locally. The differential equations for streamline trajectories and time-of-flight within the gridblock are given as

$$\frac{d\tau}{\phi} = \frac{dx}{u_x} = \frac{dy}{u_y} = \frac{dz}{u_z}. \tag{4.11}$$

To compute time of filght, consider a particle that travel from a point $(x_0, y_o, z_o)$ in the inlet cell to any point $(x_i, y_i, z_i)$ in any of the exit cell in the x, y ,z direction. The time of flight can then be obtain by integrating equation(4.11) and together with linear velociteis given in equation(4.8) is

$$\begin{aligned}
\frac{\Delta\tau_{xi}}{\phi} &= \int_{xo}^{xi} \frac{dx}{u_{xo} + c_x\left(x - x_o\right)} = \frac{1}{c_x} ln\left(\frac{u_{xi}}{u_{xo}}\right); \\
\frac{\Delta\tau_{yi}}{\phi} &= \int_{yo}^{yi} \frac{dy}{u_{yo} + c_y\left(y - y_o\right)} = \frac{1}{c_y} ln\left(\frac{u_{yi}}{u_{yo}}\right); \\
\frac{\Delta\tau_{zi}}{\phi} &= \int_{zo}^{zi} \frac{dz}{u_{zo} + c_x\left(z - z_o\right)} = \frac{1}{c_z} ln\left(\frac{u_{zi}}{u_{zo}}\right).
\end{aligned} \tag{4.12}$$

In Pollocks method, the actual cell time of fight for a particle is given as the minimum positive time of flight, that is

$$\Delta\tau = \min_{\Delta\tau > 0} \left(\Delta\tau_{x1}, \Delta\tau_{x2}, \Delta\tau_{y1}, \Delta\tau_{y2}, \Delta\tau_{z1}, \Delta\tau_{z2}\right). \tag{4.13}$$

The exit coordinate can then be found by rearranging eq (4.12)

$$\begin{aligned}
x &= x_o + u_{xo}\left(\frac{e^{c_x \frac{\Delta\tau}{\phi}} - 1}{c_x}\right) \\
y &= y_o + u_{yo}\left(\frac{e^{c_y \frac{\Delta\tau}{\phi}} - 1}{c_y}\right) \\
z &= z_o + u_{zo}\left(\frac{e^{c_z \frac{\Delta\tau}{\phi}} - 1}{c_z}\right).
\end{aligned} \tag{4.14}$$

## 4.2 Semi-analytic expression for the sensitivity

### 4.2.1 Time of flight sensitivity

Time of flight sensitivity is basic concept to obtain streamline based-calculation of the sensitivities for reservoir responses. Once time of flight sensitivities are found, it can be possible to find sensitivities that can be related to time of flight sensitivities. Therefore, it is crucial to find time of flight sensitivities first. Referring the definition of time of flight (4.7)

$$\tau = \int_{\Gamma} s(\mathbf{x}) dr,$$

where $s$ is slowness function, and it is given as

$$s(x) = \frac{\phi(\mathbf{x})}{|\mathbf{u}(\mathbf{x})|},$$

where $\mathbf{u}$ is the Darcy's velocity. By assuming that each reservoir paramter $m_i$ is constant inside grid $i$. Then, the sensitivity of time of flight $\tau$ with respect to a reservoir parameter $m_i$ along streamline $\Gamma_i$ is given as

$$\frac{\partial \tau}{\partial m_i} = \int_{\Gamma_i} \frac{\partial s(\mathbf{x})}{\partial m(\mathbf{x})}. \tag{4.15}$$

For instance, the sensitivity of time of flight $\tau$ with respect to permeablity $K_i$ along streamline $\Gamma_i$ is given in [13]

$$\frac{\partial \tau}{\partial K_i} = \int_{\Gamma_i} \frac{\partial s(\mathbf{x})}{\partial K(\mathbf{x})} = \int_{\Gamma_i} -\frac{s(x)}{k_i} = -\frac{\Delta \tau}{k_i} \tag{4.16}$$

### 4.2.2 Arrival time sensitivities

Arrival time measures the time takes a quantity to propagate from one point to a reservoir to another. As it is indicated in [3], it is possible to find the arrival time sensitivity that is related to time of flight sensitivities. In history matching problem, data is often measured at the producer(wells). Thus, it is important to compute the sensitivities of the reservoir responses at the given wells. Arrivel time sensitivities for each well $k$ can then be found by flux weighted average [1],

$$\frac{\partial t_j}{\partial m_i} = \frac{1}{\mathbf{q}} \sum_{l=1}^{N_{sl}} q_l \frac{\partial t_{j,l}}{\partial m_i}, \tag{4.17}$$

where $N_{ls}$ the total number of streamlines connected to the well and $\mathbf{q}$ is the total flux in the well.

### 4.2.3 Time-shift sensitivity

The time-shift is described in section (3.5) and, it measure for how much a simulated production curve should be shifted in time to maximaize the correlation with an observed production-response curve.The time of shift sensitivity with respect to parameter $\mathbf{m}$ is then defined as the average of the travel-time sensitivities given in (4.17) for each well $k$ is

$$\frac{\partial \Delta t_k}{\partial m_i} = \frac{1}{N_d} \sum_{j=1}^{N_d} \frac{\partial t_{k,j}}{\partial m_i}. \tag{4.18}$$

# Chapter 5

# 5 Result and discussion

## 5.1 Synthetic cases

Parameterization and pixel based methods are considered for estimation of permeability field based on the synthetic watecut data. Synthetic data is obtained from the true permeability field. In all of the examples, two phase flow of oil and water are considered. The porosity is assumed constant, $\phi$. Initially, the reservoir is saturated with oil with viscosity, 1 `centipose`. In the center of reservoir one injector is placed and starts to inject water with viscosity, 1 `centipose`. In each corner, production wells are placed in such way that, well1 is placed on the left bottom, well 2 on the right bottm, well 3 on the left top and well 4 on the right top corner of the reservoir. The pressure is set up at the producer, $\mathbf{P}_0 = 0$ and at the injecter, $\mathbf{P}_1 = 1$. One thousand streamlines are used. Different examples are considered in the following sections. Through out all examples the initial permeablity is assumed constant and plotted in **Figure** 3. In the relative and objective function figures. (The word **param** stands for paramterization method and **standard** stands for pixel method.)

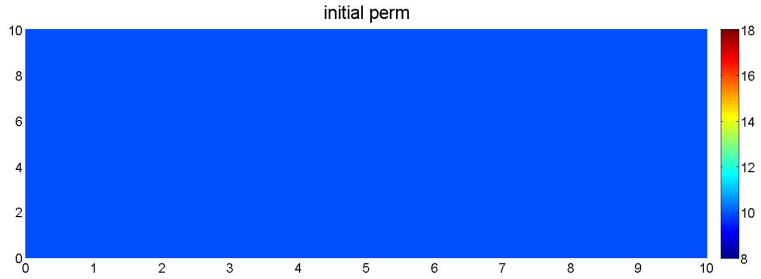


Figure 3: Initial permeability

### 5.1.1 Case 1

In this example, basis vectors that correspond to discretized Gaussian radial base function are applied on $40 \times 40$ computational grid cells. The domain size of the grid is $10 \times 10$ (dimentionless). $9 \times 9$ basis points are distributed uniformly (since we consider circular contours of basis funnctions) with parameter shape, $\sigma = 3$. Thus, 81 total sets of basis functions are possibly incorporated in the parameter estimation. This example and the next example are made to test the parametrization method as well as to compare with the pixel based method.

**Figure** 4(a) shows that the true permeability which is generated based on Gaussian radial base function with constant value. As the **Figure** 4(b) shows in parameterization method, the updated permeability field is resembles the true permeability field, eventhough it is not able to find the exact region. The norm of relative error for the parameterization method decays fast on early iteration and then it shows gradual increment see ( **Figure** 5 (top) ). This implies that there is still a small difference in the value of the premeablty field which is acceptable in reality see( the axis). In **Figure** 4(c), the updated permeability field for pixel method tries to find the region but not really match the true permeability. This is becouse of non-uniqueness of the inverse problem. That means there are different permeabilty field that can match the data exaclty. This effect clearly demonstrated in **Figure** 5 (bottom) as the objective function decreases rapidly even if, the permeablity field is not physically acceptable. In this case the relative error at the beginning tries to increase and eventually decreases.

In **Figure** 6, base vector that is used to generate true permeability field is shown. The selected base vector in **Figure** 7, is based on stepwise strategy together with performance measurement. The updated permeability in **Figure** 4(b) is the result of the refined stracture matrix. The selected base vector is resembles to the base vector that is used to generate the true permeability field. This indicates that, the performance measurement used for the selection of basis vectors has selected the best among possible sets of base vectors.

The objective function, in **Figure** 5 is plotted norm of the objective function value with respect to number of iterations. The figure shows the objective function converges for the parameterization method more early and sharply compared to standard method.

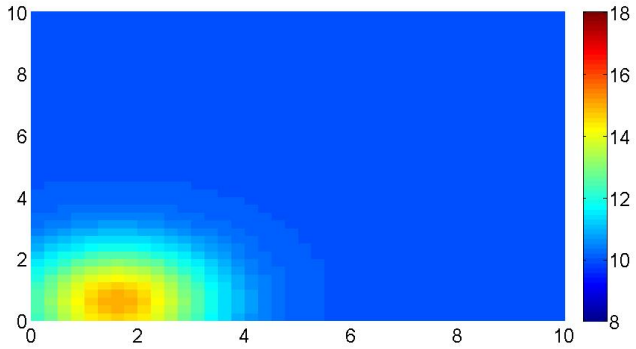


(a)

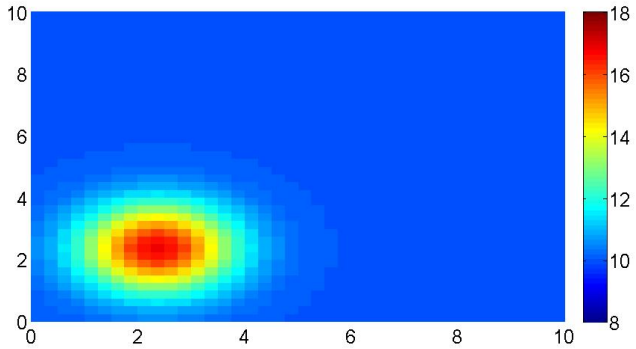


(b)

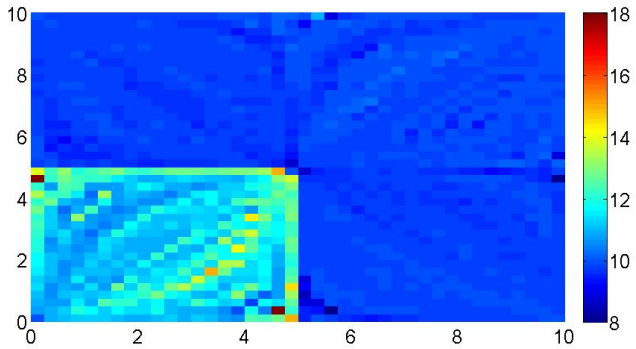


(c)

Figure 4: True Permeability (a), updated permeability based on parameteriztion method (b) and updated permeability based on pixel method (c)

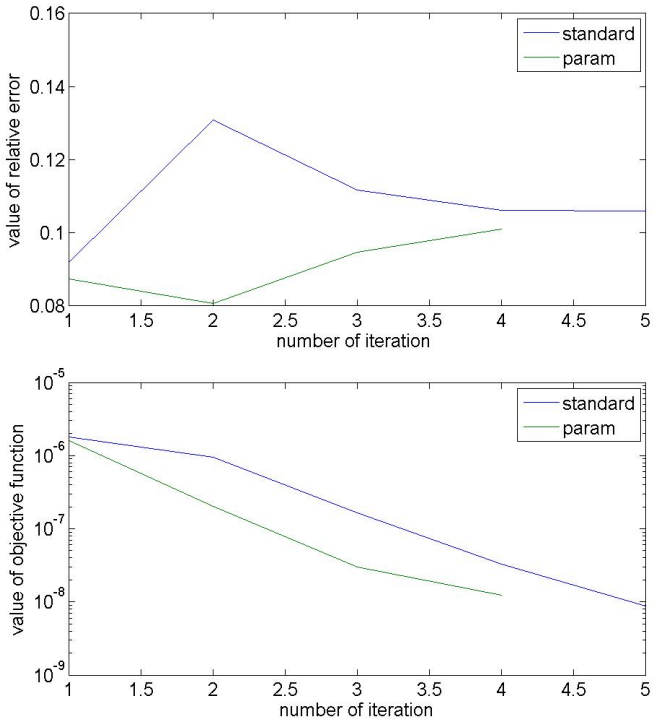


Figure 5: Relative error (top ) and objective function for time-shift (bottom) ( paramterization (green), pixel ( blue))

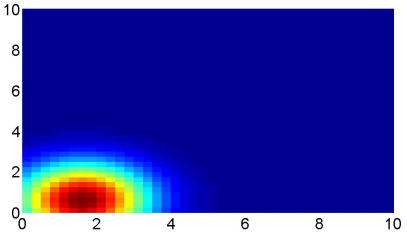

Figure 6: base vector is that is used to generate the true permeabililty

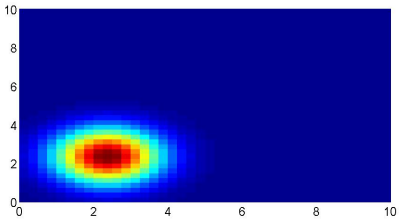

Figure 7: Selected base vector to represent to the updated permeabililty

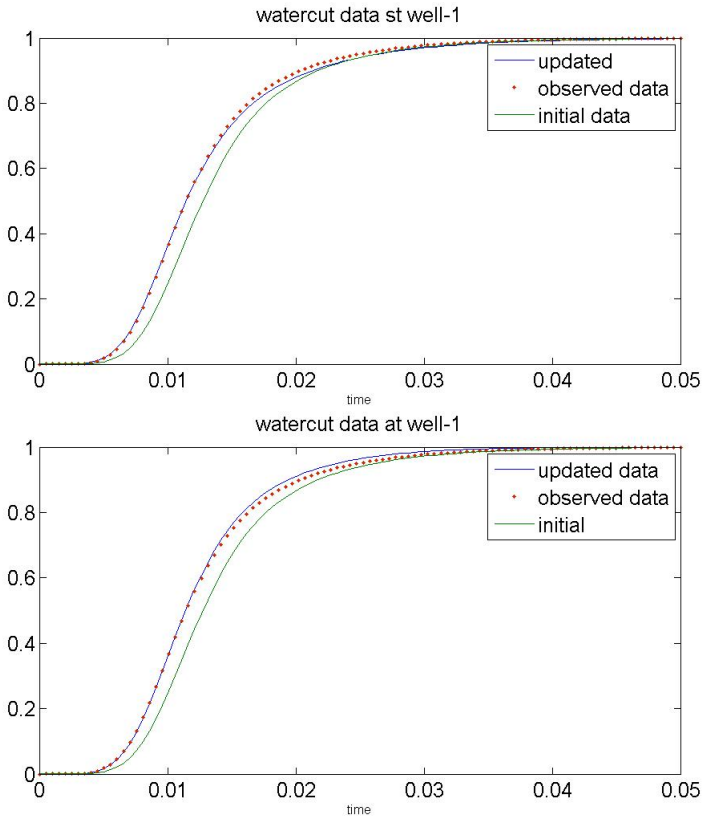


Figure 8: Watercut data resulted based on parametrization method (top) and based on pixel method (top)

In **Figure** 8 watercut data in the production wells for initial, observed and updated permeability for both methods are shown. As In **Figure** 8 clearly shows in both wells are able to match. The curve in the **Figure** 8 are resulted from injector to well 1, which is high preamble zone.

### 5.1.2 Case 2

In this case, The true permeability field is generated by combination of two base vectors and plotted in **Figure** 9(a). Twenty nine non-uniformly distributed basis points (29 total basis vectors) are possibly incorporated in the parameter estimation with the chosen parameter shape, $\sigma = 6$. All other setups are similar as previous case.

The **Figure** 9(b) shows the updated permeability field is resembles the true permeability field, but still is not able to reduce in the lower permeable zone. In **Figure** 10(a) the relative error for parameterization method decreases gradually at the beginning of iteration, and then starts increasing sharply with different slop. Looking at **Figure** 9(b), the updated permeablity in the upper corner is not a ble to find the right region compare to lower corner.

In the pixel based method, as shown in the **Figure** 9(c) the updated permeability tries to find the region, but not able to characterize the true permeability as the previous example. In this case, the relative error increases sharply and it starts decreasing. **Figure** 10(b) shows the objective function decreasing while the updated permeability are not able to characterize the permeability field as the permeability field has pixel based variation. This may lead to non-unique solution. In another way round there are a lot of possibilities to change the permeablity field which results in decreasing the objective function.

In **Figure** 10 (c) the dot points are just to show the behaviour of objective function which is resulted for each of the selected basis vectors. As it is observed, the objective function deceases until no change in the value and then shows large decreament for the selected base vector for the second time and shows finally gradual decreament for the last step.

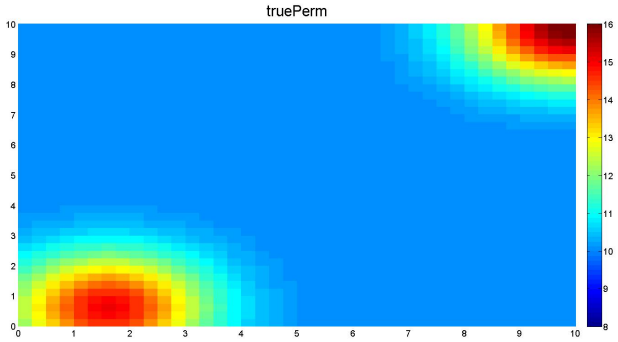


(a)

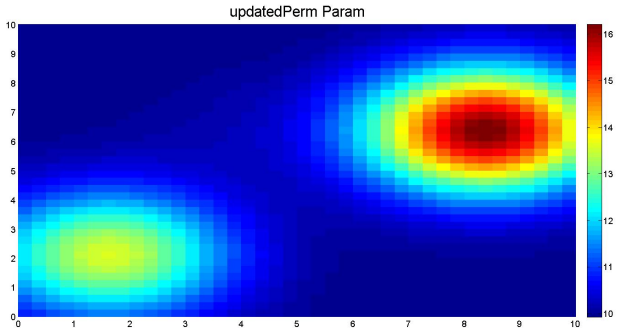


(b)

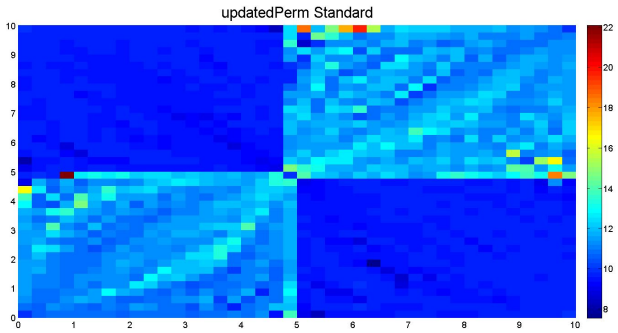


(c)

Figure 9: True permeability (a), updated permeability based on parametrization method (b) and updated permeability based on pixel method (c)

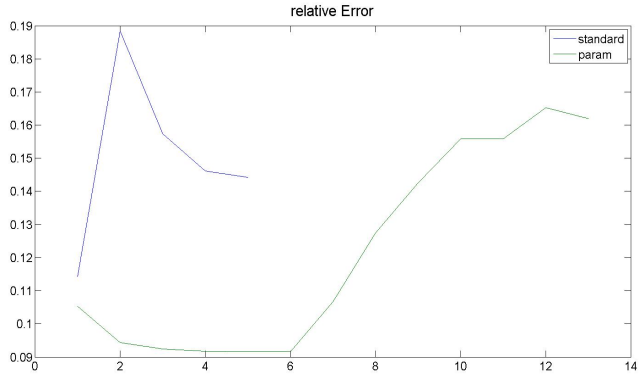


(a)

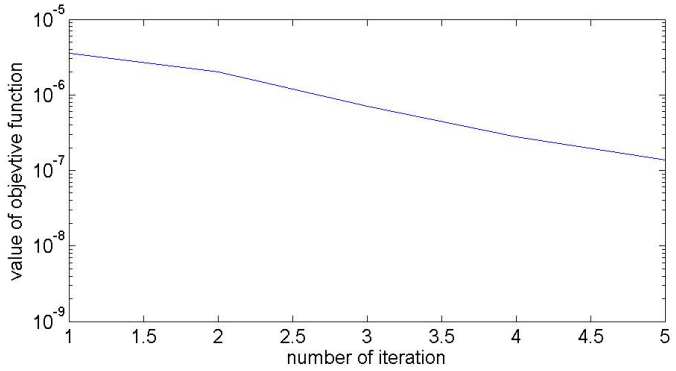


(b)

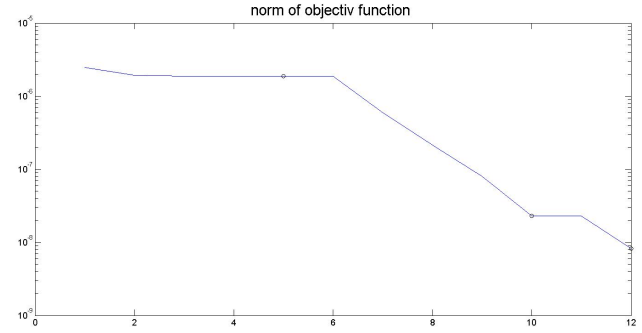


(c)

Figure 10: Relative error (a) for both method ( pixel (blue) and parameterization (blue) ), norm objective function based on pixel method (b) and norm objective function based on parameraization method (c)

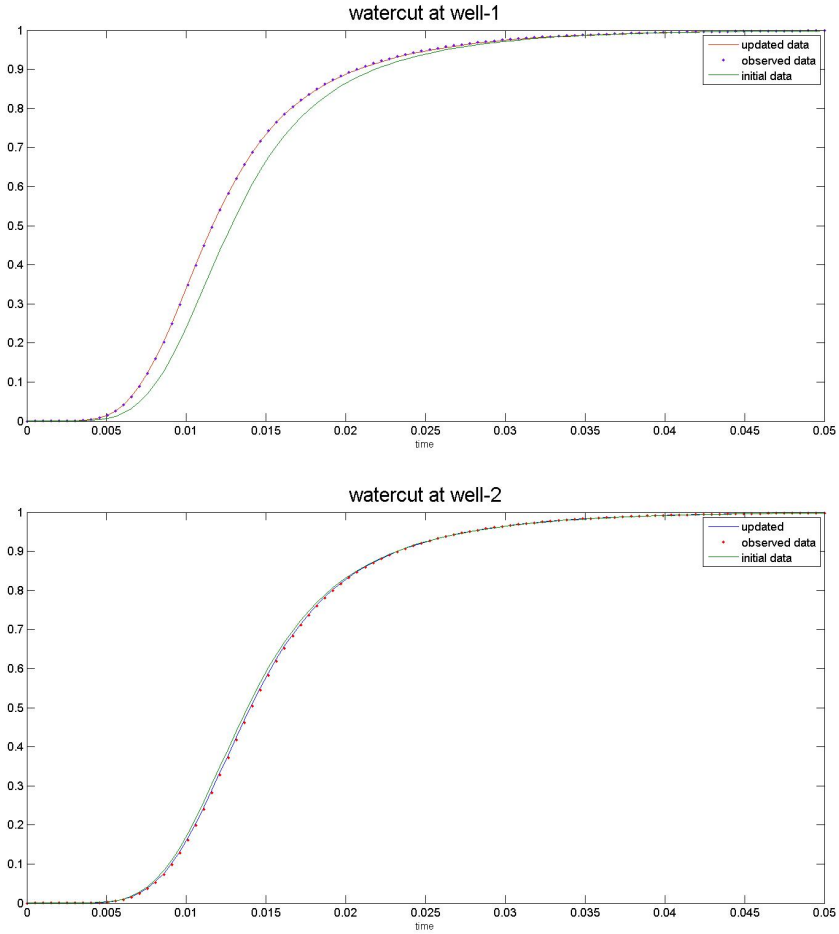


Figure 11: Watercut data at well1 and well2 resulted based on parametrization method for observed data, updated data and initial data )

.

The watercut data are able to match in both wells as in indicated in **Figure** 11.The watercut data in **Figure** 12 are able to match in both wells. Since there is no any change in permeablity field, we are not able to see any effect on the watercut data at well3. But in the pixel based method where high and law permeable zone ( well 1 and well 4 ) are not able to match as indicated in **Figure** 13 compared to the parameterization method.

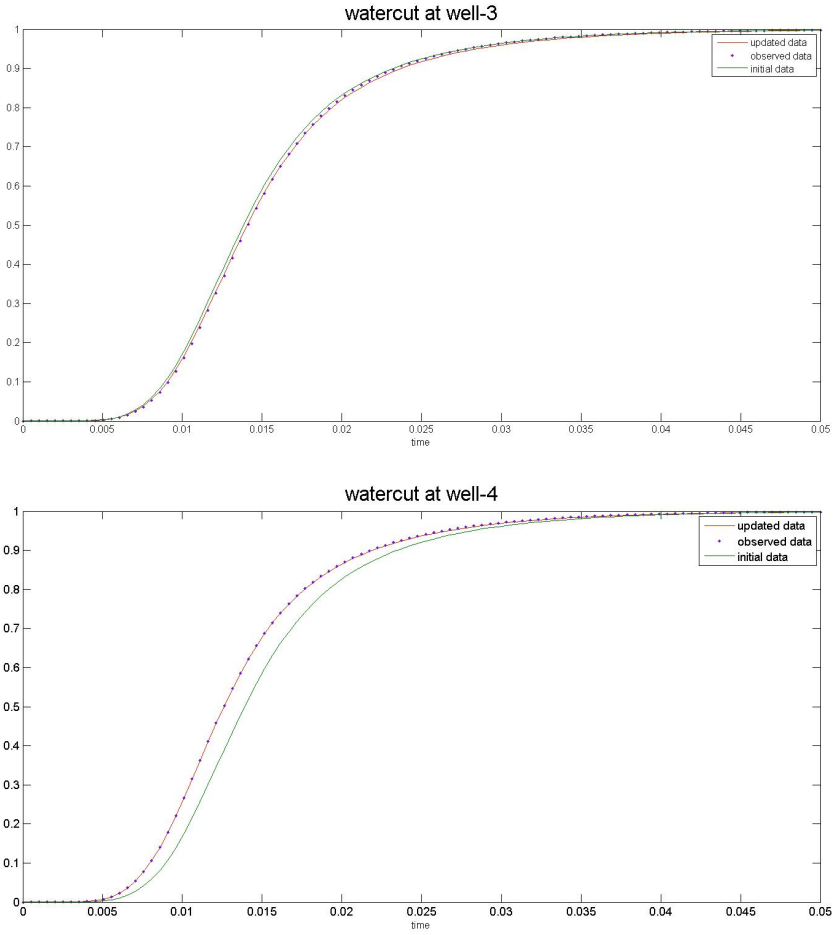


Figure 12: Watercut data at well3 and well4 resulted based on parametrization method ( observed data (blue), calculated data (red ) and initial data (green)

.

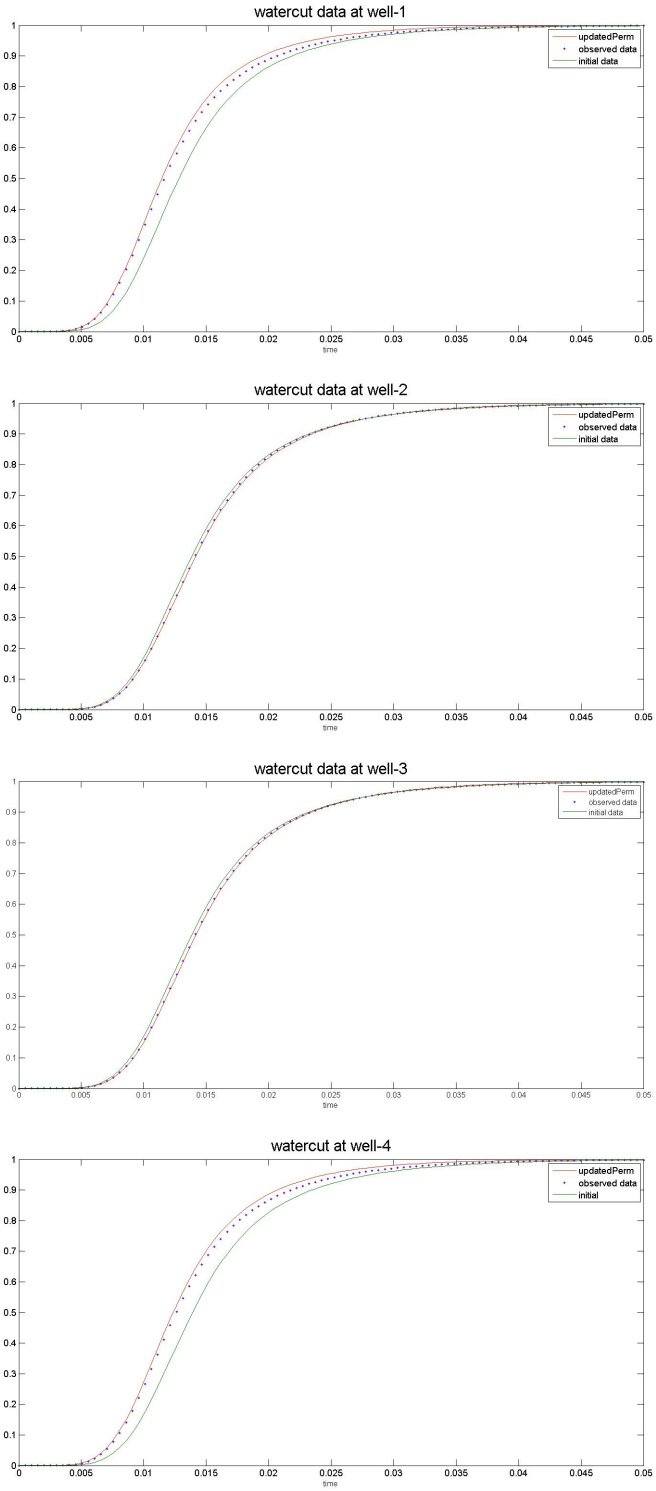


Figure 13: Watercut data resulted based on pixel method ( observed data (blue), calculated data (red ) and initial data (green) )

### 5.1.3 Case 3

As it is described in chapter 3, the permeability distribution can vary in a manner determined by the shape and support of the basis functions. To investigate the effect of the parameter shape $9 \times 9$ regularly distributed base points are considered. Therefore, 81 possible basis vectors are incorporated in the parameter estimation. Then seven different values of parameter shapes are used to analyses how the permeability field varies with respect to parameter shape. All other setups are similar to previous cases. The updated permeability field results are plotted from **Figure** 12 to 18. The distribution of these basis points are shown in **Figure** (23 ) and the true permeability field is plotted in **Figure** (14). These plots clearly show that the selection of parameter shapes has effect on variation of permeability distribution. In this particular case, the updated permeablity field that correspondes to **Figure** 13 to 16 are able to charcterize the true permeability field. But the updated permeability in **Figure** 15 and **Figure** 16 are not able to charachterize. For parameter shape values of $\sigma = 1$ and $\sigma = 2$ the basis vectors are not able to identify the pereambility field since it covers very small area. In case of parameter shape 7 it covers very large area as indicated in **Figure** ( 18)

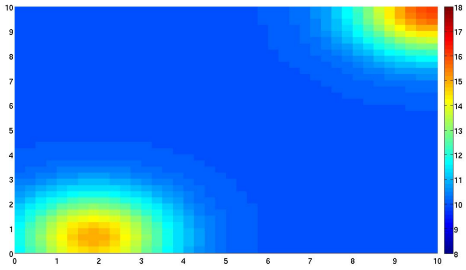

Figure 14: True Permeability

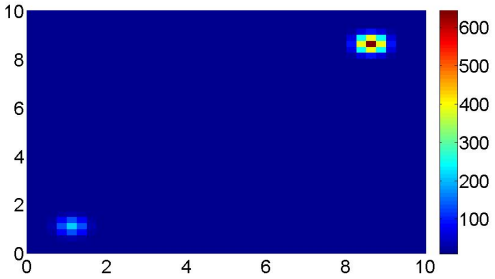


Figure 15: Updated permeability for $\sigma = 1$

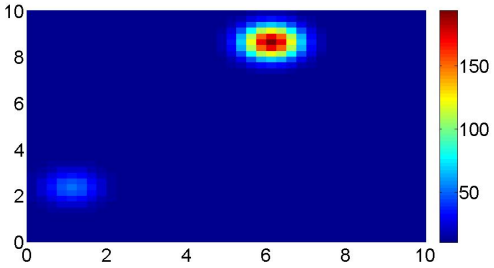


Figure 16: Updated permeability fro $\sigma = 2$

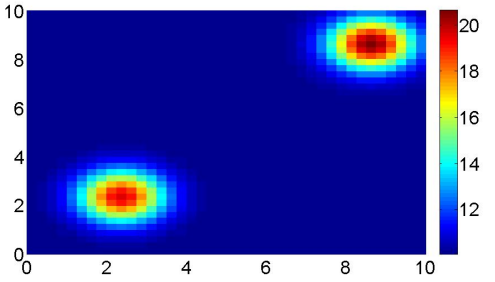


Figure 17: Updated permeability for $\sigma = 3$

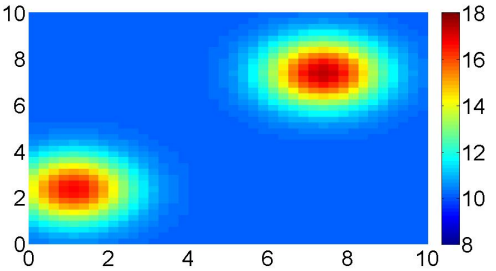


Figure 18: Updated permeability for $\sigma = 4$

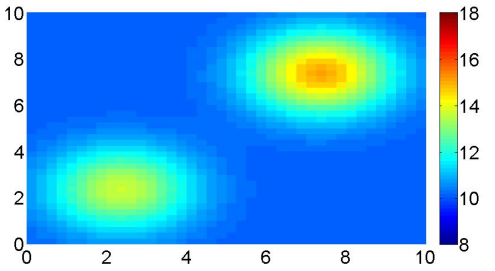


Figure 19: Updated permeability for $\sigma = 5$

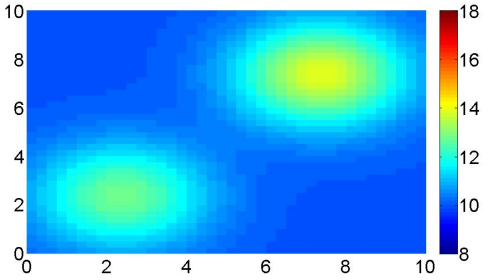


Figure 20: Updated permeability for $\sigma = 6$

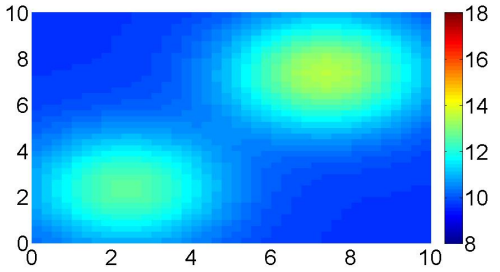


Figure 21: Updated permeability for $\sigma = 7$

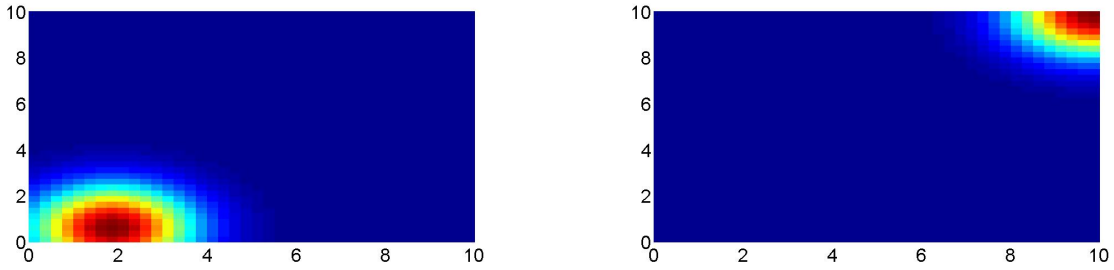


Figure 22: basis vectors used to generate true permeability

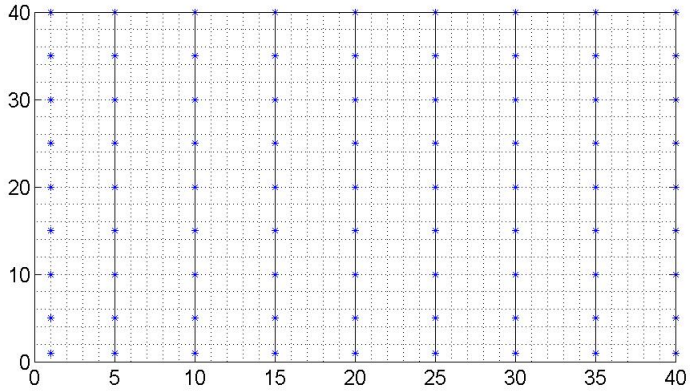


Figure 23: The distibuted basis points (81)

The basis vectors that is used to generate the true permeabiltiy field are plotted in **Figure** 22 and the uniformly distributed basis points are plotted in **Figure** 23.

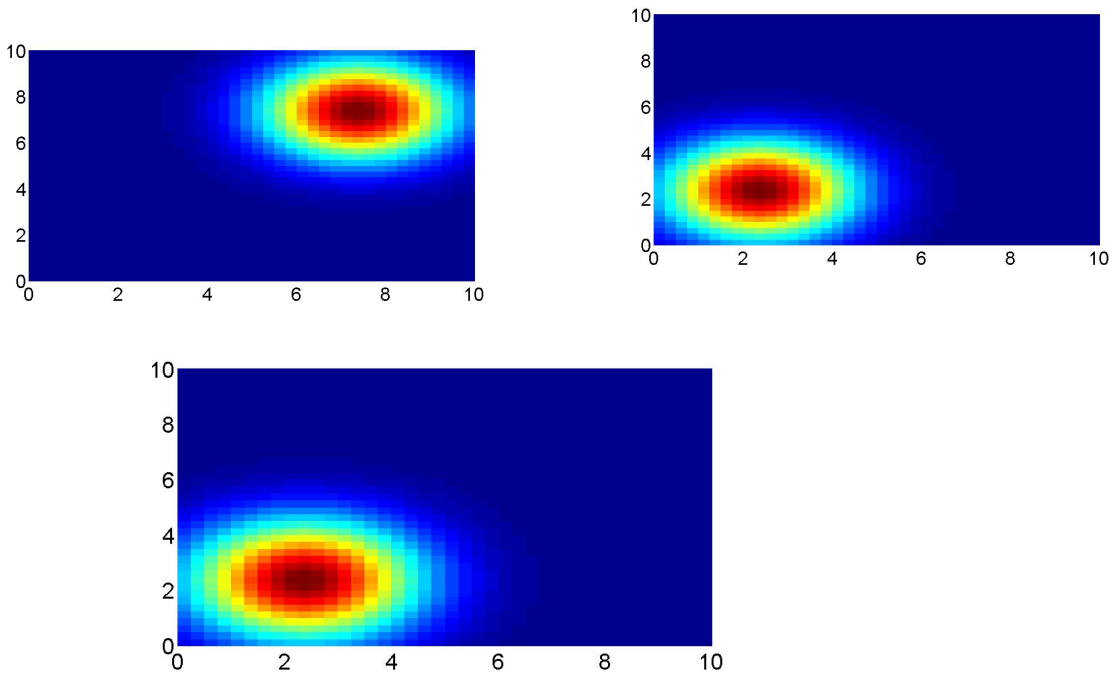


Figure 24: The selected base vector in the first step (top left), The selected base vector in the second step (top right) and The selected base vector in the third step (bottom)

**Figure** 24, shows the selected basis vectors at each step. The updated permeability in **Figure** (20) is the result of the combination of the selected basis vectors. The selected basis vectors are resembles to the basis vectors in **Figure** 22 that are used to generate the true permeability even though they are not in the right region.

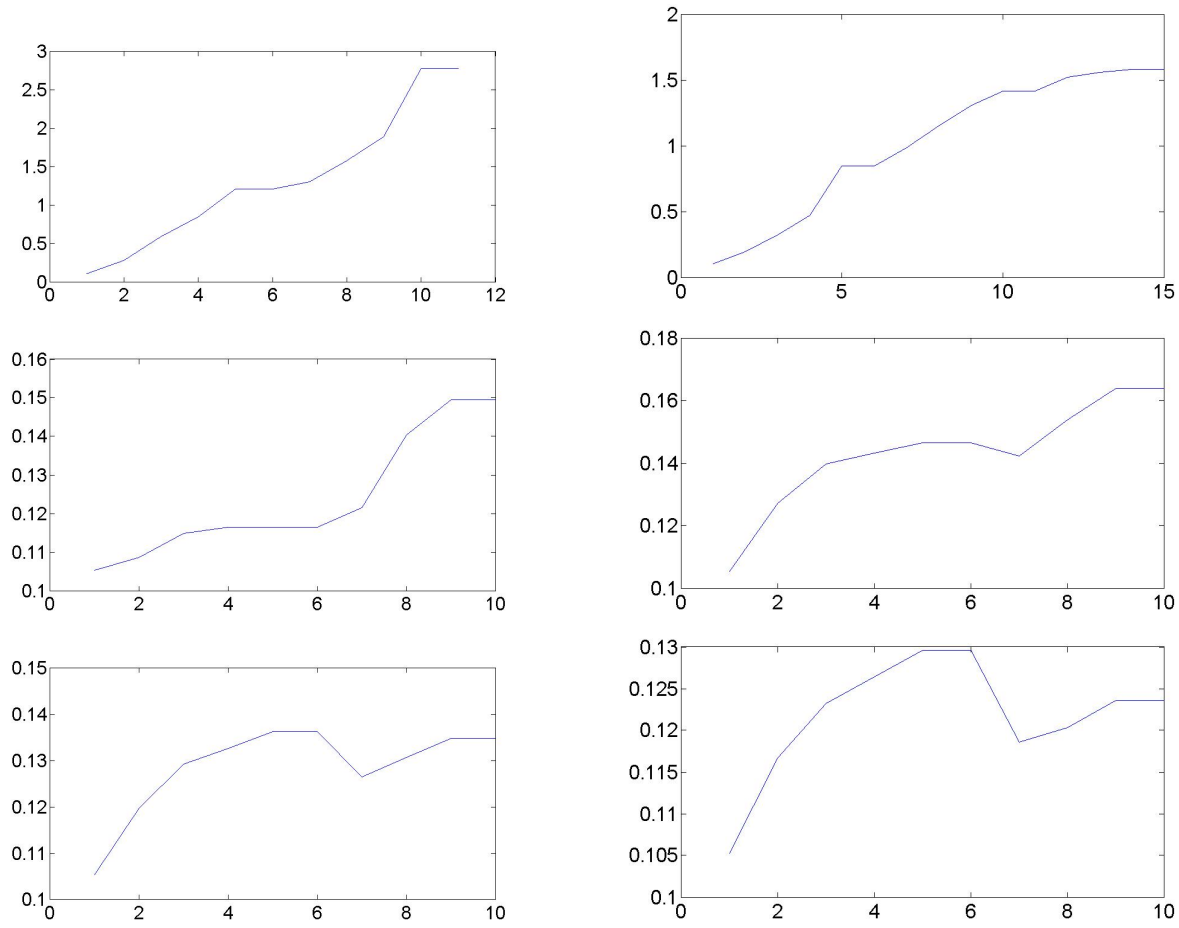


Figure 25: Relative error for $\sigma = 1$(top left), for $\sigma = 2$ (top right), for $\sigma = 3$ (middle left), for $\sigma = 4$ (middle right), for $\sigma = 5$ ( bottom left), for $\sigma = 6$ (bottom right)

The norm of relative errors that corrosponds to each $\sigma$ with respect to number of iteration are plotted on **Figure** 25. The norm of relative error for all value of $\sigma$ are shown increament, but the value of relative error for $\sigma = 1$ and $\sigma = 2$ that corresponds to the updated permeability field in **Figure** 15 and **Figure** 16 resepectively are higher than the rest. This is the reason that, the values of updated permeability for parameter shapes $\sigma = 1$ and $\sigma = 2$ have great discrepancy as it is observed from the axis.

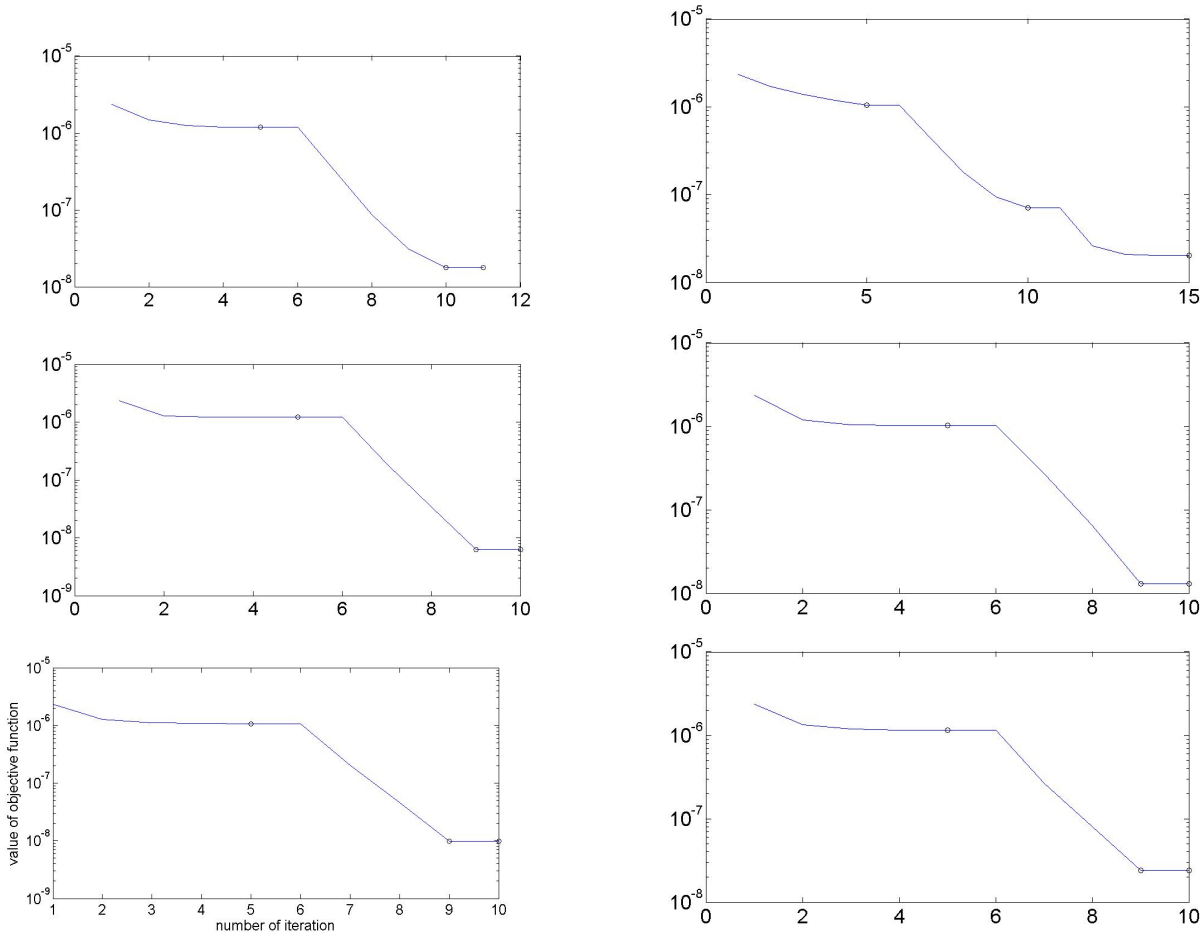


Figure 26: norm of objective function for time-shift for $\sigma = 1$(top left), for $\sigma = 2$ (top right), for for $\sigma = 3$ (middle left), for $\sigma = 4$ (middle right), for $\sigma = 5$ ( bottom left), for $\sigma = 6$ (bottom right)

The behavoir of the objective function for time-shift that related to different paramter shape are plotted in **Figure** 26. All these figures shows approximalty the same perforamnce in sense of reducing the the objective function. All of the objective function converges at early iteration compare to objective function for the case where $\sigma = 2$,

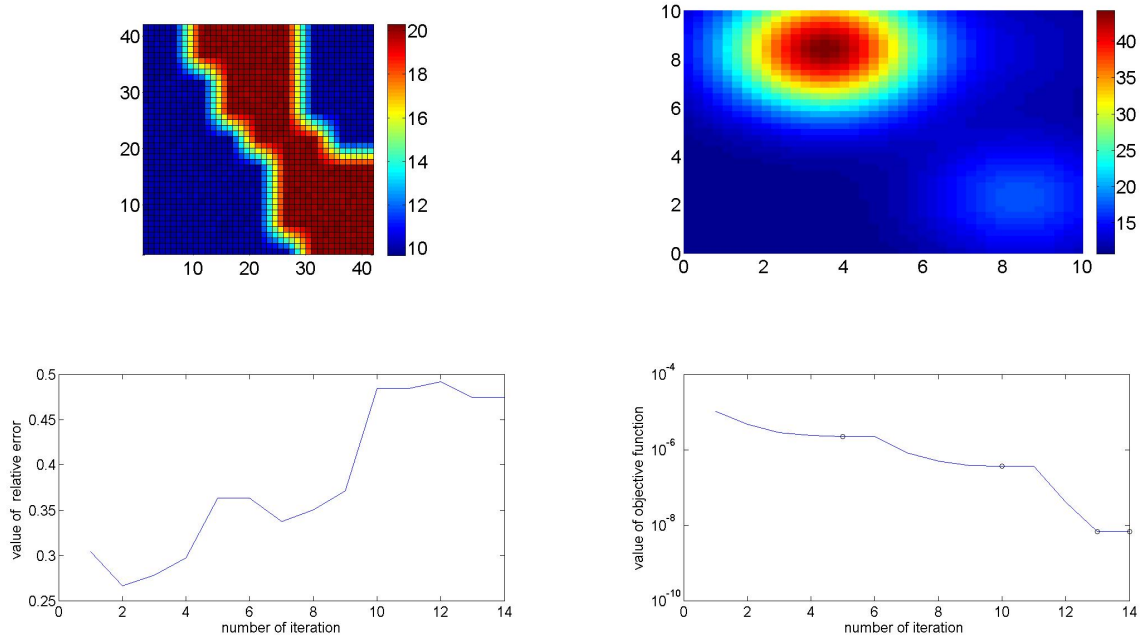


Figure 27: True permeability (top left), updated permeability (top right), relative error (bottom left) and norm of objective function for time-shift (bottom right)

### 5.1.4 Case 4

In this example, basis vectors that correspond to discretized Gaussian radial base function is applied on $41 \times 41$ computational grid cells. The possible basis vectors are the same as the previous case 3. The chosen parameter shape is, $\sigma = 7$.

The true and updated permeability field are plotted in **figure** (27) (top left) and **figure** 27 (top right) respectively. The high-permeable distribution in true permeability field trends from north west to south east. As **figure** 27 ( top right) indicates that the permeability field is able to find the region, but not able to characterize the permeability field. The relative error in **figure** 27 (bottom left) is increasing in each of iteration while the behaviour of objective function is decreasing in all of the selected basis vectors see **Figure** 27 (bottom right)

The definition and formulation of time-shift sensetivity are clearly persented in section (4.2.3). This concept is cleary shown in **figure** 28. The watercut data and sensitivity based on both initial and updated permeability are plotted in **Figure** 28.). It is reasonable to get lower sensitivity in high permeable region of the updated permeability field as indicated in **Figure** 27 (top right). The watercut data in well1 are not able to observe any change except very small difference at the beginning of the production curve. This is cleary manifested in the senstivity plotes as we are able to observe very small change near in the area of injecter well. The watercut data are able to match perfectly in well3 compare to well2 and well4. This is due to sensitivity at upper left corner for updated permeability is quite uniform and lower compare to the other. Thus, the time takes to shift the calculated production curve was earlier than the other. Infact the watercut data at well 2 and 3 are alse able to match in a good way.

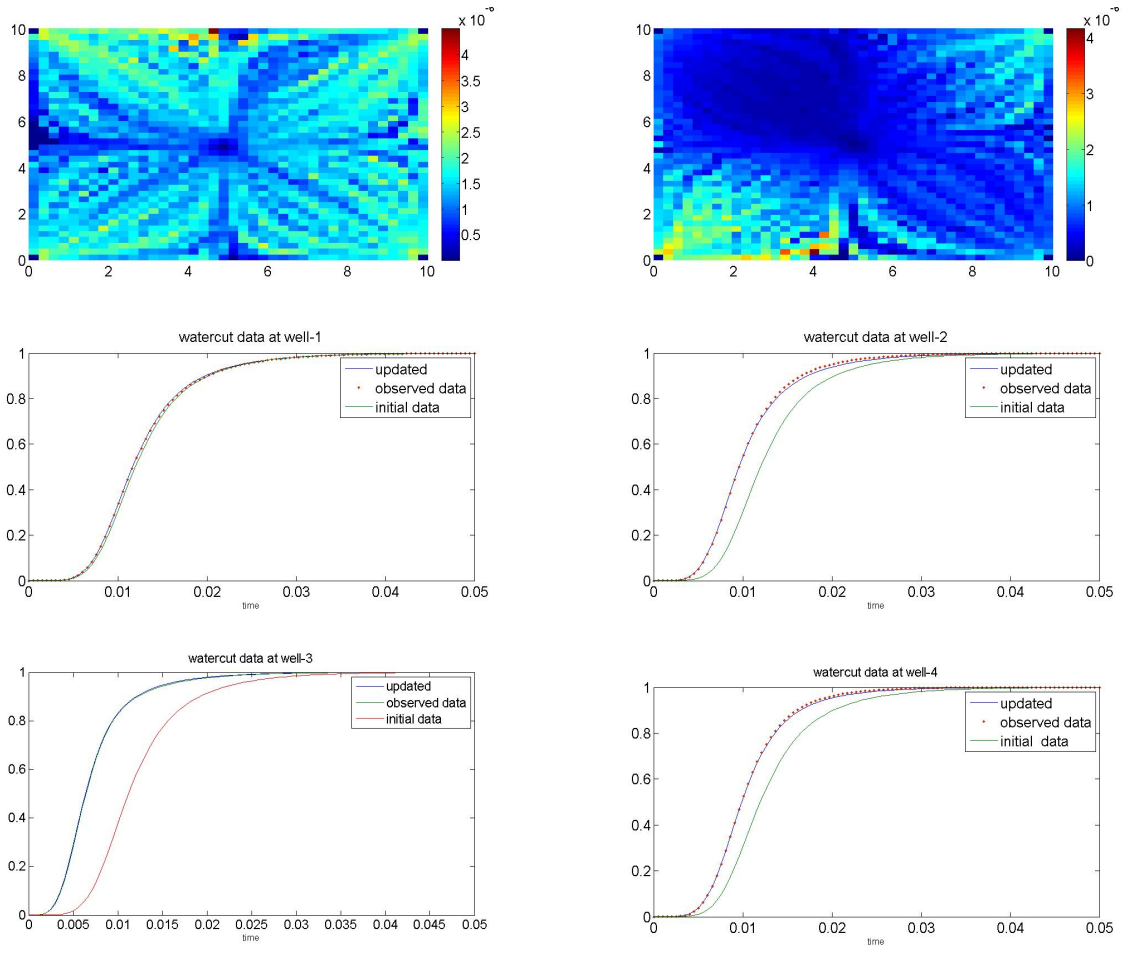


Figure 28: Sensitivity based initial permeability (top left), sensitvity based on updated permeability (top right),watercut data at well1 (middle left), watercut data at well2 (middel right), watercut data at well3 (bottom left) and watercut data at well4 (bottom right)

## 5.2 Conclusion and recommendation

The main purpose of this thesis was to investigate history matching with reduced parameterizaton. The purpose of reduced parameterizaton was to regularize the inverse problem encountered in history matching. Regularization by parameterization was implemented in this work. The parameterization structure was updated sequentially by using stepwise strategy.

The simulation results in case 1 and case 2 demonstrated, parameterization method performs well in terms of characterizing permeability field and minimizing the objective function compared with pixel based method. For pixel based method, indicated the property of non-unique problem. As the permeability field has pixel based variation, there are usually many parameters that are equally good in approximately matching the data which may lead to unphysical estimation.

Then the effect of parameter shape on parameterization method was investigated in case 3. The simulation results showed that the selection of parameter shape has effect in a sense of characterizing permeability field.

The last case, the simulation results showed that the updated permeability tried to find the region, but it did not able to characterize the true permeability field. This is due to limited amount of avaliable information as it is only watercut data is considerd.

Generally the method has improved the non-unique problem and was able to give expected result for the simple test cases. Due to the complexity of history matching problem, the regularization method was not able to improve the performance of ill-posed for the last case.

In this work, objective gradient base function is applied for the performance measure. But linearization of model response can also be applied to investigate the effect of the performance measurement. In addition considering more information and prior knowledge can be used to improve the results.

# Nomenclature

| Symbol | Description |
|---|---|
| $\alpha$ | fluid phase |
| $\alpha$ | step length |
| $\Delta t_k$ | time-shift at well k |
| $\Delta_k$ | trust- region radius |
| $\Gamma$ | the path of streamline |
| $\lambda$ | trust-region parameter |
| $\lambda_\alpha$ | mobility of phase |
| $\mu$ | viscosity in centipose |
| $\phi$ | porosity |
| $\Psi$ | Stream function in 2D |
| $\psi, \chi$ | Bi-Stream function in 3D |
| $\rho$ | density in $kg/m^3$ |
| $\tau$ | time of flight |
| $\xi$ | arc-length |
| $d_j^{cal}$ | calculated data $j$ |
| $d_j^{obs}$ | observed data $j$ |
| $F$ | fractional flow of water |
| $f$ | objective function |
| $i, l$ | cell indexes |
| $k$ | well index |
| $k_w$ | relative permeability for the wetting phase |
| $k_{nw}$ | relative permeability for the non-wetting phase |
| $m$ | size of model space |
| $n$ | size of data space |
| $N_d$ | number of data points |
| $N_w$ | number of wells |
| $N_{sl}$ | number of streamlines |
| $p$ | pressure in Pa |
| $Pc$ | capillary pressure |
| $G$ | flow rate from source or sink in $m^2/day$ |
| $S$ | saturation of water |
| $s(x)$ | slowness function |
| $t$ | time |
| $t_k^{cal}$ | calculated reference time at well $k$ |
| $t_k^{obs}$ | observed reference time at well $k$ |
| $w_j$ | weight of data $j$ |
| $d$ | data vector |
| $D^k$ | diagonal scaling matrix |
| $G$ | linear forward operator |

| | |
|---|---|
| $g$ | gravitational acceleration constant |
| $I$ | identity matrix |
| $\mathbf{r}$ | residual vector |
| $\mathbf{u}$ | the Darcy velocity in $m/day$ |
| $\mathbf{P}$ | Permeability field |
| $\mathbf{S}$ | stractural matrix |
| $\mathbf{C}$ | Coefficient vector |
| $\sigma$ | Parameter shape |
| $\Gamma$ | amplication factor |
| $B$ | basis points |

# References


[1] Tor Harald Sandve. *Streamline based History Matching.* Master thesis, May 8, 2009.

[2] Jacob Bear. *Dynamics of fluids in porous media.* American Elseviser Publishing Company, Inc, 1972. ISBN 0-444-00114-X.

[3] Akhil Datta-Gupta and Michael J.King. *Streamline Simulation: Theory and Practice.* Society of Petroleum Engineers, 2007. ISBN 978-1-55563-111-6.

[4] Inga Berre. *Fast Simulation of Transport and Adaptive Permeability Estimation in Porous Media.* Doctor Scientiarum Thesis. 2005.

[5] I. BERRE, F. CLMENT, M. LIEN and T. MANNSETH. *Data driven reparameterization structure for estimation of fluid conductivity.* Research Paper, 2007.

[6] Akhil Datta-Gupta Hao Chang and Zhong He. *A comparison of travel-time and amplitude matching for field-scale production-data integration: Sensitivity,non linearity, and practical implication.* SPE 84570, 2005.

[7] Zhong He Hao Chang, Arun Kharghoria and Akhil Datta-Gupta. *Fast history matching of finite-difference models using streamline-derived sensitivities.* SPE 89447, 2005.

[8] Dean S. Oliver Yan Chen. *Recent progress on reservoir history matching: a review.* Comput Geosci (2011) 15:185221.

[9] D.W. Vasco, Seongsik Yoon, and Akhil Datta-Gupta. *Integrating Dynamic Data Into High-Resolution Reservoir Models Using Streamline-Based Analytic Sensitivity Coefficients.*SPE Journal 4 (4), December 1999.

[10] Randall J. LeVeque. *Finite Difference Methods for Differential Equations*, 1998.

[11] Jorge Nocedal and Stephen J. Wright.*Numerical optimization.* Springer, 1999. ISBN 0-387- 98793-2.

[12] Brian Borchers Richard C. Aster and Clifford H. Thurber. *Parameter Estimation and Inverse Problems.* American Elseviser Publishing Company, Inc, 2004. ISBN 0-12-065604-3.

[13] V.R.Stenerud.*Streamline-based history matching.* PhD thesis, Norwegian University of Science and Technology, 2007.

[14] K.-A.Lie V.R.Stenerud, V.Kippe and A.Datta-Gupta. *Adaptive Multiscale Streamline Simulation and Inversion for High-Resolution Geomodels.* Society of Petroleum Engineers, 2007.

[15] K.-A.Lie V.R.Stenerud, V.Kippe and A.Datta-Gupta. *Multiscale-Streamline Simulation and dynamic data integration for High-Resolution subsurface models.* 2007.

[16] Guanren Huan Zhangxin Chen and Yuanle Ma. *Computational Methods for Multiphase Flows in Porous Media.* Society for Industrial and Applied Mathematics, 2006. ISBN 0-89871-606-3.